sustainability

MDPI

Article

Estimated Population Exposure Within Designated Hazard Zones Across Walkability-Based Urban Spatial Characteristics in Japan: A Nationwide Analysis of Postcode-Level Population Core Cells

Keisuke Utsu * and Osamu Uchida

Department of Information Media Technology, School of Information Science and Technology, Tokai University, Hiratsuka 259-1292, Japan; o-uchida@tokai.ac.jp

* Correspondence: utsukei@tokai.ac.jp

Abstract

While Japan's population is declining overall, some areas remain densely populated within designated hazard zones. Understanding how these spatial patterns vary across urban contexts is important for sustainable and resilient urban development. This study presents a nationwide analysis of hazard-specific estimated population exposure at postcode-level population core cells across walkability-based urban spatial characteristics in Japan. We integrated designated hazard-zone layers from the Geospatial Information Authority of Japan (GSI) with 250 m census population grids and linked the resulting dataset to the Japan Postcode-level Walkability Index using these core cells as a common spatial unit. This analysis used postcode-level population core cells and was not designed to estimate total hazard-zone-based exposure within entire postcode areas. The four hazard-zone layers were analyzed separately to characterize hazard-specific patterns, not to assess simultaneous or compound hazard events, cumulative exposure, or compound risk. Population core cells in higher-JPWI strata generally overlapped more frequently with flood, storm surge, and tsunami inundation zones, whereas lower-JPWI population core cells overlapped more frequently with designated landslide warning zones. Where hazard-zone overlap was identified, estimated exposed populations tended to be larger in higher-JPWI core cells. The pattern should be interpreted descriptively because the estimate is partly influenced by cell population and JPWI includes a population-density component. Overall, the results show hazard-specific differences in how walkability-based urban spatial characteristics coincide with hazard-zone-based estimated population exposure, providing a transparent and nationally consistent baseline for characterizing designated hazard-zone overlap and estimated exposed population at population core cells in Japan.

Keywords: disaster prevention; natural disasters; hazard information; walkability; estimated exposed population

Check for updates

Academic Editors: Jianming Cai, Qiang Zhang, Lei Xu, Biao Hu and Jiann-Wen Woody Ju

Received: 3 June 2026
Revised: 26 June 2026
Accepted: 30 June 2026
Published: 4 July 2026

Copyright: © 2026 by the authors. Licensee MDPI, Basel, Switzerland. This article is an open access article distributed under the terms and conditions of the Creative Commons Attribution (CC BY) license.

1. Introduction

A variety of natural hazards, including river flooding, storm surges, tsunamis, and landslides, occur in Japan, and their impacts have become more evident due to climate change, urban development, and urbanization. The scale of damage is shaped not only by the magnitude and frequency of hazards but also by the number of people living in affected areas and the urban environment in which they conduct their daily lives. In Japan, while the overall population has been declining nationwide in recent years, some disaster-prone

areas have continued to attract or retain population. This highlights the need to characterize nationwide patterns and associations among urban spatial characteristics, hazards, and population distribution.

Walkability provides one perspective for describing urban spatial characteristics. In urban planning and public health research, walkability is commonly discussed in relation to population density, land-use or facility diversity, street connectivity, proximity to daily life destinations, and pedestrian accessibility. These walkability-related characteristics are relevant not only to everyday mobility and urban sustainability but also to disaster preparedness, because they are associated with where people live, how populations are concentrated, and how residents may access local facilities and evacuation-related information. Accordingly, examining hazard-zone overlap and estimated exposed population across walkability-based urban spatial contexts can provide useful baseline information for sustainable and resilient urban development.

From the perspective of hazard exposure, existing studies have analyzed population exposure to natural hazards at multiple spatial scales. At the global level, satellite observations have revealed an increasing trend in population exposure to climate-related hazards such as floods, with urbanization and changes in residential locations identified as drivers of increased exposure [1]. Efforts have also been made to evaluate simultaneous exposure to multiple climate-related hazards, and an increase in multi-hazard exposure has been reported [2]. In Japan, nationwide analyses covering earthquakes, tsunamis, storm surges, floods, and landslides have integrated social vulnerability and population exposure at the sub-municipal level [3]. Studies have estimated current population exposure to floods and other hazards using Population Census data [4]. In addition, long-term increases and decreases in exposure have been projected at a nationwide scale while accounting for future population scenarios and climate change [5]. These studies show the importance of analyzing population exposure to natural hazards at broad spatial scales. However, to interpret such exposure in relation to everyday urban environments, it is also useful to consider walkability-based urban spatial characteristics using a consistent national framework.

Focusing on populations and households within designated flood inundation zones, prior work reports that despite nationwide population decline, residential development within such areas has led to increases in population and the number of households [6]. It has also been pointed out that nationwide population growth within designated flood inundation zones is largely driven by in-migration into Urbanization Promotion Areas [7]. Regarding evacuation, studies have estimated the number of people requiring evacuation during heavy rain events by considering flood and landslide warning zones together with building stories, at both national and prefectural levels [8]. In addition, for catchment zones of designated evacuation centers in Yokohama City, research has integrated multiple hazard datasets and population information and classified zone characteristics via cluster analysis [9].

To operationalize these walkability-based urban spatial characteristics, walkability has been assessed through objective indicators of urban form, including density, land-use mix, intersection density, proximity to destinations, and accessibility [10–12]. However, conventional walkability indices developed mainly for Western cities may not fully capture the characteristics of high-density Asian cities [13]. In Japan, the Japanese Walkability Index (JWI) has been proposed as a walkability indicator developed for Japanese cities [14], and its validity as an explanatory measure of walking behavior has been examined using large-scale step-count data in Yokohama [13]. Furthermore, the Japan Postcode-level Walkability Index (JPWI) has been developed at the postcode scale for all of Japan, integrating three components within a 1 km walking catchment: population density, the number of types of daily life facilities, and street connectivity [15,16].

Research on walkability in relation to disaster risk and hazard information remains limited [17]. A comparative study across multiple Baltic Sea coastal cities discusses the potential compatibility of walkability and flood resilience in waterfront public spaces [18]. In Japan, a case study of Susaki City, Kochi Prefecture, argues on conceptual and qualitative grounds that walkability should be considered in the context of disaster risk [19], although the analysis focused on a single city. An analysis of the Tokyo metropolitan area shows that both walkability and disaster risk affect housing preferences, suggesting that the interaction between topography, convenience, and safety shapes urban structure [20]. Relatedly, a case study of post-2011 Great East Japan Earthquake collective relocation areas indicates that steep terrain increases the walking burden for older adults, affecting both daily convenience and safety [21]. These studies provide important insights into population exposure, evacuation planning, and walkability-related urban environments. However, no nationally consistent analysis has yet linked JPWI-defined urban spatial characteristics with multiple designated hazard-zone layers and estimated exposed population using postcode-level population core cells as a common spatial unit. This gap limits the ability to characterize how walkability-based urban spatial contexts coincide with designated hazard zones and estimated population exposure in a comparable nationwide framework. Addressing this gap is also relevant to international frameworks that emphasize both sustainability and disaster risk reduction, such as SDG 11 ("Make cities and human settlements inclusive, safe, resilient and sustainable") [22] and the Sendai Framework for Disaster Risk Reduction from 2015 to 2030 [23].

To address this gap, this study aims to establish a nationwide analytical framework that integrates JPWI, hazard-zone layers, and 250 m population grid data using postcode-level population core cells as a consistent spatial unit. In this study, "exposure" is operationally defined as hazard-zone-based estimated population exposure derived from spatial overlap between population core cells and designated hazard-zone layers. This definition does not represent hazard probability, expected event frequency, event likelihood, or expected loss. This framework supports a systematic nationwide characterization of hazard-specific estimated population exposure across JPWI-defined urban spatial contexts in Japan. Using this approach, we examine differences in (i) hazard inclusion frequency, (ii) areal overlap, and (iii) estimated exposed population across JPWI strata.

This study makes three contributions. First, it provides a nationwide, walkability-stratified characterization of hazard-zone-based estimated population exposure for four hazard types at postcode-level population core cells in Japan. Second, it establishes a nationally consistent and reproducible analytical framework that integrates hazard-zone layers, JPWI as a nationwide walkability index, and population distribution, thereby enabling comparable characterization across urban spatial contexts. Third, it shows, within this common framework, that the observed patterns of hazard-zone overlap and estimated exposed population across JPWI strata differ by hazard type rather than following a uniform pattern across all hazards. Taken together, these contributions provide a nationally consistent and reproducible descriptive baseline for characterizing designated hazard-zone overlap and estimated exposed population for four hazard types examined separately across walkability-based urban spatial characteristics in Japan. This baseline is intended as a population core-cell-based descriptive characterization, rather than as a test of causal mechanisms or an estimate of total hazard-zone-based exposure within entire postcode areas.

2. Materials and Methods

This section describes the data and analytical workflow. In this study, we analyze the following hazard types available on the Hazard Map Portal Site provided by the Geospatial Information Authority of Japan (GSI) [24]:

- Flood inundation (planned scale, L1);
- Storm surge inundation (maximum assumed scale);
- Tsunami inundation (maximum assumed scale);
- Landslide warning zones (including designated zones for debris-flow, steep-slope failure, and landslide).

We exclude layers for designated areas where buildings are at high risk of collapse due to flood flow or riverbank erosion because their damage mechanisms differ from the other hazards analyzed. We also exclude inland flooding and snow-avalanche warning layers because nationwide coverage in the GSI hazard tiles is incomplete, which limits national-scale comparability. Figure 1 presents the overall analytical flow.

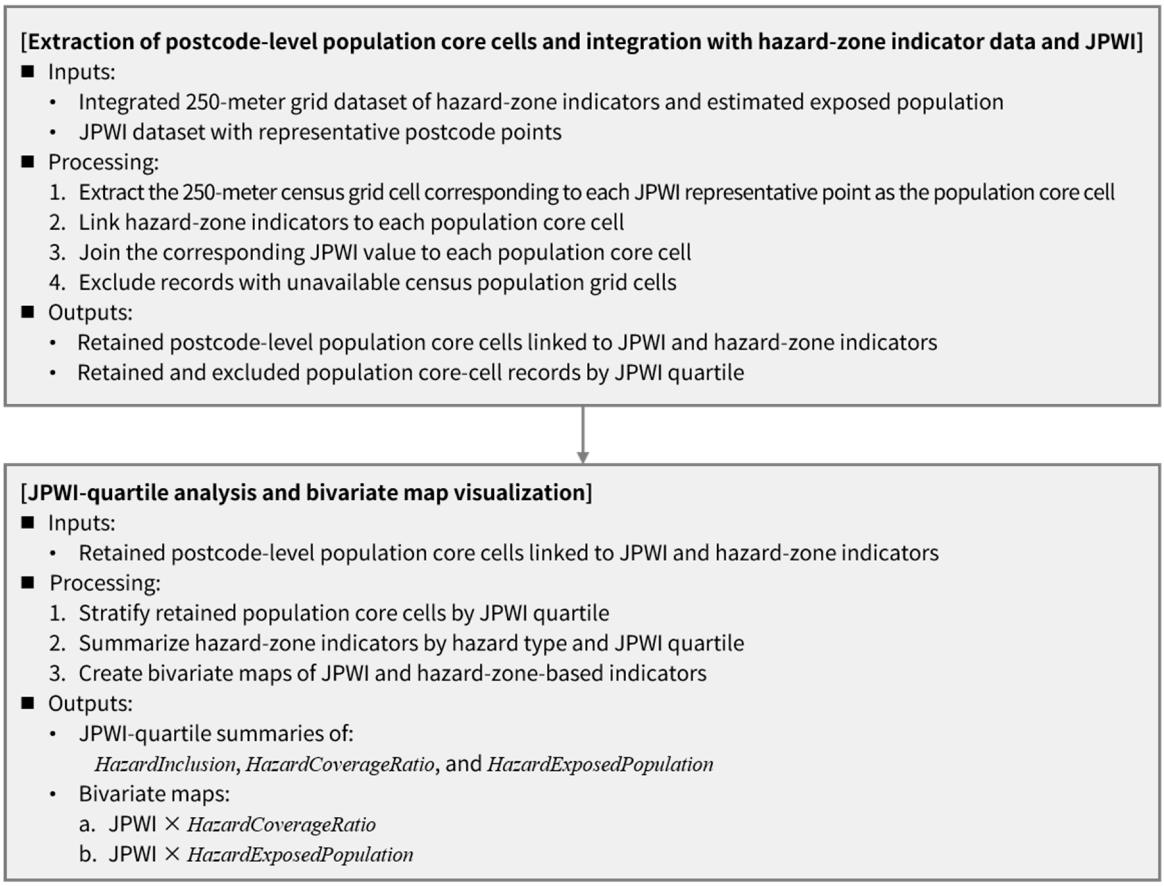


Figure 1. Main analytical workflow for extracting postcode-level population core cells and summarizing JPWI-stratified hazard-zone indicators.

2.1. Input Data

2.1.1. Integrated 250 m Grid Dataset of Hazard-Zone Overlap and Estimated Exposed Population

We use a nationwide Japan 250 m grid dataset that represents hazard-zone overlap and estimated exposed population. The dataset was developed by integrating hazard-zone layers from the GSI Hazard Map Portal [24] with the 2020 Population Census 250 m grid [25] and is publicly available on Zenodo [26]. In this dataset, exposure is operationally represented by spatial overlap with designated hazard-zone layers and by the estimated

population within those overlapping areas. This operational definition does not represent hazard probability, expected event frequency, event likelihood, or expected loss. The GSI hazard-zone layers differ in data availability and spatial coverage depending on hazard type and responsible authority. Therefore, the absence of identified hazard-zone pixels in a grid cell does not necessarily mean that the cell is free from hazard. It may also reflect the absence of an available source layer for that location. Because explicit and nationally consistent coverage masks were not available for all hazard-zone layers, this study did not construct an approximate coverage proxy, as doing so could introduce additional uncertainty and arbitrary assumptions. The hazard-zone layers used in this study were retrieved on 31 January 2026.

Table 1 summarizes the scenario or designation, coverage limitations, and interpretation of the hazard-zone layers used to construct the integrated 250 m grid dataset. All hazard-zone layers were obtained from the GSI Hazard Map Portal as raster tiles, and hazard pixels were summarized within 250 m Population Census grid cells to calculate *HazardInclusion*, *HazardCoverageRatio*, and *HazardExposedPopulation*. Because the hazard layers differ in scenario assumptions, designation criteria, and spatial coverage, the analysis was designed to characterize JPWI-stratified patterns separately for each hazard type, rather than to directly compare hazard severity or risk levels between hazard types.

Table 1. Characteristics and interpretation of designated hazard-zone layers used to construct the integrated 250 m grid dataset of hazard-zone overlap and estimated exposed population.

Hazard-Zone Type	Scenario/Designation	Coverage Limitation	Interpretation/Analytical Use
Flood inundation zones	Planned scale (L1). Both planned-scale and maximum-assumed-scale flood layers are available as open data; this study used the planned-scale layer because it represents a more frequent scenario.	Availability and spatial coverage vary by responsible authority.	Identify population core cells overlapping with planned-scale flood inundation zones.
Storm surge inundation zones	Maximum assumed scale.	Primarily limited to coastal areas; preparation and publication are not uniform across all coastal regions and responsible authorities.	Identify population core cells overlapping with maximum-assumed storm surge inundation zones.
Tsunami inundation zones	Maximum assumed scale.	Primarily limited to coastal areas; availability varies by responsible authority.	Identify population core cells overlapping with maximum-assumed tsunami inundation zones.
Landslide warning zones	Designated warning zones for debris-flow, steep-slope failure, and landslide; warning and special-warning classes were not distinguished.	Coverage and designation status vary by responsible authority; warning and special-warning classes were not distinguished in this study.	Identify population core cells overlapping with designated landslide warning zones.

Note: All hazard-zone layers were obtained from the GSI Hazard Map Portal as raster tiles and summarized within 250 m Population Census grid cells. Because the hazard layers differ in scenario assumptions, designation criteria, and spatial coverage, the indicators were interpreted separately for each hazard type and were not used to compare absolute hazard severity or risk levels directly across hazard types.

For landslide-related hazards, three types of zones are defined in Japan: debris-flow, steep-slope failure, and landslide. Consistent with the dataset specification, these three zone

types are combined into a single binary indicator (presence/absence) using the union of the debris-flow, steep-slope failure, and landslide layers, without distinguishing between yellow (warning) and red (special-warning) classes. This unified binary indicator was used to characterize whether a population core cell overlapped with any designated landslide-related warning zone, rather than to estimate landslide hazard severity or regulatory status. We hereafter refer to this unified indicator as landslide warning zones.

For each 250 m grid cell i and hazard type h, the dataset provides the following indicators:

- $HazardInclusion_{i,h}$ (0/1): This is 1 if at least one raster pixel within grid cell i is classified as a hazard zone; otherwise, it is 0. Because the published hazard layers do not cover all areas uniformly nationwide, $HazardInclusion = 0$ indicates that no hazard-positive pixel was identified in the available hazard-zone layer for that cell. It should not be interpreted as definitive absence of hazard, a complete estimate of hazard absence, or confirmation that the cell is outside all possible hazard areas.
- $HazardCoverageRatio_{i,h}$ (ranges from 0.000 to 1.000): The ratio of cell i covered by the hazard, calculated as the ratio of hazard pixels to total pixels in grid i.

$$HazardCoverageRatio_{i,h} = \frac{N_{i,h}^{exposed}}{N_i^{total}}$$

$N_{i,h}^{exposed}$: The number of raster pixels within grid cell i that fall inside the hazard zone of type h.

N_i^{total}: The total number of raster pixels contained within grid cell i.

- $HazardExposedPopulation_{i,h}$: The estimated exposed population in each 250 m grid cell, calculated by multiplying the census population ($CellPopulation_i$) of the cell by $HazardCoverageRatio_{i,h}$.

$$HazardExposedPopulation_{i,h} = CellPopulation_i \times HazardCoverageRatio_{i,h}$$

2.1.2. Walkability Index (JPWI)

The Japan Postcode-level Walkability Index (JPWI) [15,16] defines a representative point for each postcode area as the center coordinate of the 250 m grid cell with the largest population. In this study, this cell is referred to as the population core cell. JPWI is calculated within a 1 km network-based walking catchment from each postcode representative point by integrating population density, the diversity of daily life facilities, and street network connectivity. It therefore captures urban spatial characteristics beyond population density alone and can be used to characterize urban environments consistently across Japan. JPWI is available for 113,156 postcode areas across Japan. Figure 2 shows the histogram of JPWI values. The ranges, counts, and percentages of JPWI quartiles are summarized in Table 2. Figure 3 presents the spatial distribution of JPWI quartiles in the Tokyo metropolitan area. The national distribution of JPWI quartiles and the supplementary component-level summary by JPWI quartile are provided in Appendix A, Figure A1 and Table A1, respectively.

Table 2. Sample size in each JPWI quartile in the original JPWI dataset.

JPWI Quartile	JPWI Interval	Original JPWI Records, *n*	Percentage (%)
Q1	[−1.848, −0.806)	28,289	25.0%
Q2	[−0.806, 0.041)	28,289	25.0%
Q3	[0.041, 0.764)	28,289	25.0%
Q4	[0.764, 2.589]	28,289	25.0%
Total		113,156	100.0%

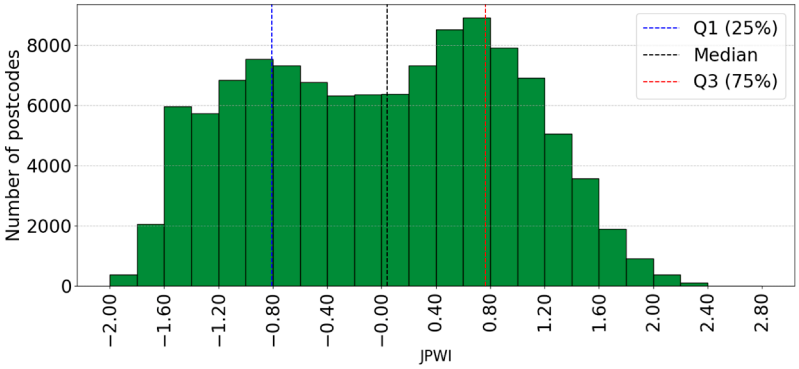


Figure 2. Histogram of JPWI values for all postcode areas in Japan.

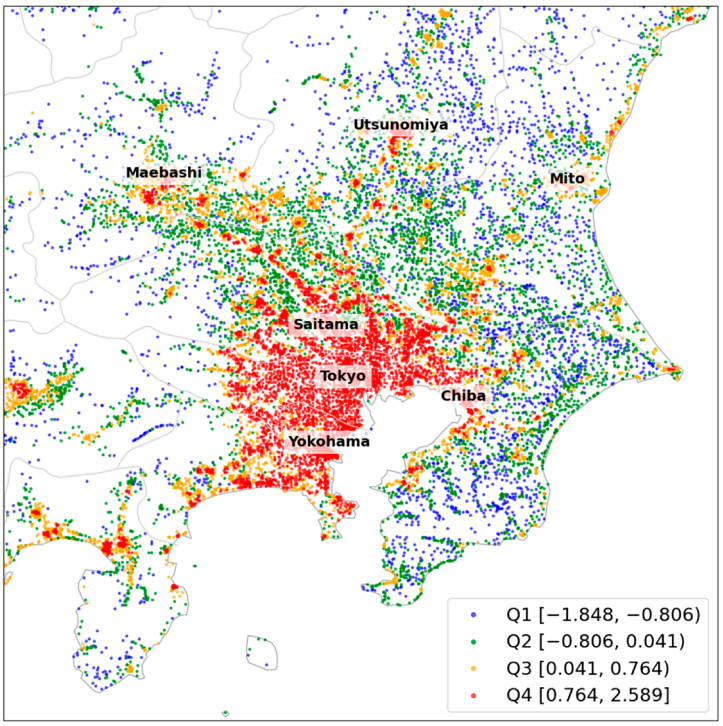


Figure 3. Distribution of JPWI quartiles at population core cells in the Tokyo metropolitan area.

2.2. Extraction of Postcode-Level Population Core Cells and Integration with JPWI

For each postcode area, we extracted the 250 m census grid cell corresponding to the representative point provided in the JPWI dataset and used it as the population core cell. This population core cell approach was used to ensure spatial consistency with the JPWI representative point, which is defined as the center coordinate of the most populous 250 m grid cell within each postcode area. JPWI values and the integrated 250 m grid dataset of hazard-zone overlap and estimated exposed population (Section 2.1.1) were linked to these core cells. Because JPWI is defined for postcode areas using this representative point, rather than as an area-wide average of walkability across the entire postcode area, using the corresponding population core cell was necessary to maintain spatial consistency between JPWI and the 250 m grid-based hazard-zone indicators. An analysis using all populated 250 m cells or entire postcode areas would require either treating JPWI as an area-wide proxy or recalculating walkability-related indicators for alternative spatial units, thereby changing the analytical unit and scope of the present study. Therefore, the present approach characterizes hazard-zone overlap and estimated exposed population at postcode-level population core cells and was not designed to estimate total hazard-zone-based exposure within entire postcode areas.

After excluding postcode areas for which the corresponding 250 m census grid cell was unavailable because of confidentiality-related suppression, the final analysis sample comprised 106,230 postcode-level population core cells. Table 3 shows the number of original JPWI records, retained population core cells, excluded records, and retention rates by JPWI quartile. Excluded records correspond to JPWI records whose representative 250 m census population grid cells were unavailable because of confidentiality-related suppression. The overall retention rate was 93.9%, although the retention rate was lower in Q1 than in the other quartiles. Nevertheless, the retained sample included 23,226 population core cells in Q1 and more than 27,000 cells in each of Q2–Q4. Therefore, the original JPWI quartile thresholds were retained to ensure consistency with the published JPWI dataset, while the potential influence of confidentiality-related exclusion, particularly in Q1, is acknowledged as a limitation.

Table 3. Retained and excluded postcode-level population core cells by JPWI quartile.

JPWI Quartile	JPWI Interval	Original JPWI Records, *n*	Retained Core-Cell Records, *n*	Excluded Records, *n*	Retention Rate (%)
Q1	[−1.848, −0.806)	28,289	23,226	5063	82.1%
Q2	[−0.806, 0.041)	28,289	27,030	1259	95.5%
Q3	[0.041, 0.764)	28,289	27,787	502	98.2%
Q4	[0.764, 2.589]	28,289	28,187	102	99.6%
Total		113,156	106,230	6926	93.9%

Note: Original records indicate postcode areas included in the published JPWI dataset. Retained core-cell records indicate records for which the corresponding representative 250 m census population grid cell was available and linked to the hazard-zone indicator dataset. Excluded records indicate original JPWI records whose corresponding representative 250 m census population grid cells were unavailable because of confidentiality-related suppression. Retention rate was calculated as retained records divided by original JPWI records.

Quartile cut points were defined using the original JPWI dataset and then applied to classify the retained sample. The processed analysis subset used in this study, which includes postcode-level population core cells and indicators of hazard-zone overlap and estimated exposed population, has been deposited on Zenodo and is publicly available [27]. JPWI values are not included in this repository because they are part of a separately published dataset created by other authors.

2.3. Quartile-Stratified Analysis and Bivariate Map Visualization

Population core cells were stratified into JPWI quartiles (Q1–Q4). For each JPWI quartile and hazard type, we summarized the dataset-derived indicators as follows: (i) the proportion of core cells with *HazardInclusion* = 1, (ii) the distribution of *HazardCoverageRatio* among cells with *HazardInclusion* = 1, and (iii) the distribution of *HazardExposedPopulation* among cells with *HazardInclusion* = 1. For *HazardInclusion*, the proportion was calculated using all retained population core cells in each JPWI quartile as the denominator. These proportions indicate the share of retained population core cells in which hazard-positive pixels were identified in the available hazard-zone layers. They should not be interpreted as complete estimates of hazard presence or absence, because explicit and nationally consistent coverage masks were not available for all hazard-zone layers.

For bivariate mapping of *HazardCoverageRatio* and *HazardExposedPopulation*, JPWI quartiles were grouped into three categories: Q1, Q2–Q3, and Q4. Each hazard indicator was also reclassified into three quartile-based categories: Q1, Q2–Q3, and Q4, using thresholds derived separately for each hazard type from the national distribution of population core cells with *HazardInclusion* = 1. These JPWI and hazard-indicator categories were combined in a 3 × 3 bivariate scheme. Because the thresholds were defined separately for each hazard type and indicator, the bivariate maps are intended to support within-hazard interpretation

of spatial co-distribution patterns, not direct comparison of absolute areal overlap or the magnitude of estimated exposed population across different hazard types. Maps for the Tokyo metropolitan area are presented in the main text, whereas nationwide maps are provided in Appendix B.

2.4. Supplementary Diagnostic, Sensitivity, and Descriptive Analyses

As a supplementary diagnostic analysis, we compared hazard-zone indicators calculated using postcode-level population core-cell records with those calculated using all populated 250 m census grid cells in selected case-study regions. This comparison was conducted to examine how the population core-cell representation differs from an all-populated-cell representation within selected regional contexts. The comparison was used only as a diagnostic check and was not designed to replace the nationwide core-cell analysis or to provide a comprehensive region-specific exposure assessment. Because JPWI is defined for postcode representative points rather than for all populated 250 m census grid cells, the all-cell comparison was not conducted as a JPWI-stratified analysis. The detailed procedure and results are reported in Appendix C.

As a supplementary local-neighborhood sensitivity analysis, we calculated hazard-zone indicators using the population core cell itself and the surrounding grid cells with available census population data within a 3 × 3-cell neighborhood centered on each postcode-level population core cell. This analysis was conducted to examine whether the JPWI-stratified patterns observed in the main core-cell analysis were sensitive to the use of only the representative population core cell. For each population core cell and hazard type, we calculated the proportion of these cells with *HazardInclusion* = 1, the mean *HazardCoverageRatio*, and the sum of *HazardExposedPopulation* across these cells. These local-neighborhood indicators were then summarized by JPWI quartile. JPWI quartiles were assigned based on the JPWI value of the postcode representative point corresponding to the central population core cell and were not recalculated for the 3 × 3 neighborhood. This analysis was not intended to estimate total hazard-zone-based exposure within entire postcode areas, because the 3 × 3 neighborhood does not necessarily correspond to postcode boundaries. The results are reported in Appendix D.

As a supplementary descriptive analysis, we also counted, for each population core cell, the number of hazard-zone types for which *HazardInclusion* = 1. This count was used to characterize cases in which multiple hazard-zone types were identified within the same population core cell in the available hazard-zone layers. It does not represent simultaneous hazard occurrence, compound hazard processes, cumulative exposure, or multi-hazard risk. The resulting counts and percentages are reported in Appendix E Table A4, and the detailed combinations are reported in Appendix E Table A5.

2.5. Computational Environment and Use of Generative AI Tools

Generative AI tools were used as auxiliary tools for computational workflow support and manuscript preparation. Google Colaboratory (Google Colab; Google LLC, Mountain View, CA, USA) with Python 3.12.13 was used for data analysis and figure preparation. Google Gemini (Gemini 3 Flash; Google LLC, Mountain View, CA, USA; used in March–May 2026) was used to assist in generating and revising Python code snippets for data analysis and figure preparation. The generated code was manually reviewed, modified where necessary, executed by the authors, and verified against the input datasets and intermediate outputs. ChatGPT (GPT-5.5 Thinking; OpenAI, San Francisco, CA, USA; used in March–June 2026) and Microsoft 365 Copilot (Think Deeper mode; Microsoft Corporation, Redmond, WA, USA; used in March–June 2026) were used to support AI-assisted language checking and wording refinement. The generative AI tools were used only as auxiliary

tools; the final analytical workflow, results, interpretation, and manuscript content were determined and verified by the authors. All AI-assisted outputs were manually reviewed and verified by the authors.

3. Results

This section presents the results of a descriptive national-scale analysis based on the nationally consistent framework described above, focusing on broad patterns of estimated population exposure at population core cells across hazard types and walkability-based urban spatial characteristics.

3.1. Hazard-Zone Inclusion Frequency by JPWI Quartiles

Figure 4 presents the proportion of population core cells in which at least one hazard-positive pixel was identified for each hazard type, stratified by JPWI quartiles. For flood inundation, the proportions of core cells with *HazardInclusion* = 1 in Q2–Q4 (0.351–0.391) were consistently higher than in Q1 (0.190), indicating that population core cells in higher JPWI quartiles overlapped more frequently with flood inundation zones than those in Q1. Although storm surge and tsunami inundation zones are geographically concentrated in coastal areas and thus exhibit lower absolute proportions, both hazards show an increasing trend in hazard inclusion with higher JPWI quartiles. In contrast, landslide warning zones display the opposite pattern: the proportion of included population core cells decreases with higher JPWI quartiles. Because explicit and nationally consistent coverage masks were not available for all hazard-zone layers, the reported *HazardInclusion* proportions should be interpreted as the proportion of retained population core cells in which hazard-positive pixels were identified in the available official hazard-zone layers. These proportions should not be interpreted as complete estimates of hazard presence or absence.

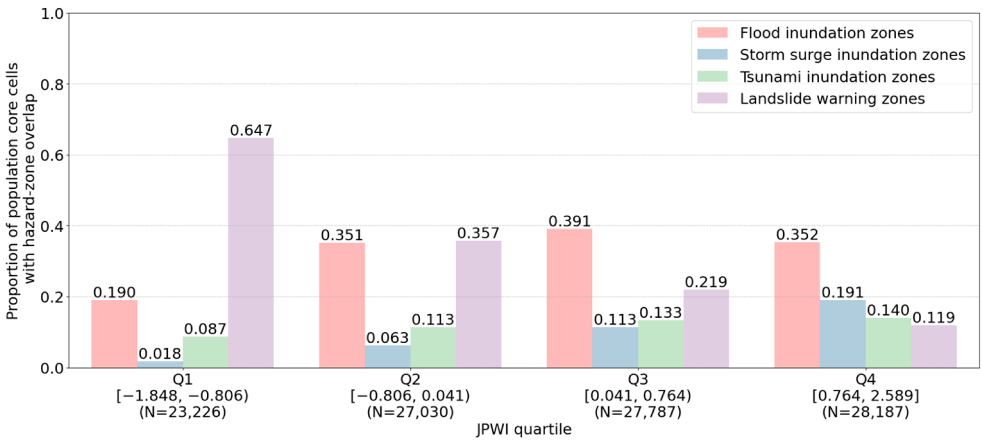


Figure 4. Proportion of retained population core cells with *HazardInclusion* = 1 by hazard type and JPWI quartile. Percentages were calculated using the number of retained population core cells in each JPWI quartile as the denominator; N indicates the number of retained population core cells in each quartile. The reported percentages represent identified overlap in the available official hazard-zone layers and should not be interpreted as complete estimates of hazard presence or absence. *HazardInclusion* = 0 indicates that no hazard-positive pixel was identified in the available hazard-zone layer and should not be interpreted as definitive absence of hazard.

3.2. Areal Overlap with Hazard Zones by JPWI Quartiles

3.2.1. Distribution of Areal Overlap (Boxplots)

Figure 5 shows boxplots of *HazardCoverageRatio* for population core cells with *HazardInclusion* = 1, stratified by JPWI quartiles. The number of included cells and descriptive statistics are reported in Table 4. In the boxplots, whiskers represent the minimum

and maximum values within 1.5 times the interquartile range (IQR) from the first and third quartiles; outliers are not shown. For flood, storm surge, and tsunami inundation, both the median and upper-end values of *HazardCoverageRatio* tend to increase with higher JPWI quartiles. Conversely, for landslide warning zones, higher JPWI quartiles show lower medians and narrower distributions, suggesting that overlap with designated landslide warning zones was more extensive among low-JPWI population core cells.

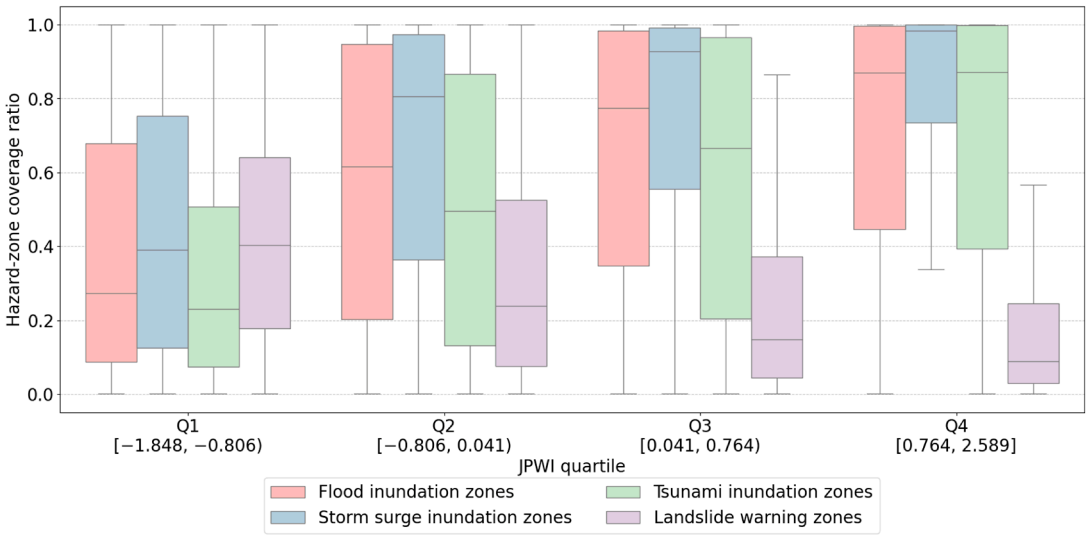


Figure 5. Distribution of *HazardCoverageRatio* by JPWI quartile among population core cells with *HazardInclusion* = 1. Outliers are not shown for readability. Descriptive statistics are reported in Table 4.

Table 4. Hazard inclusion frequency and descriptive statistics of *HazardCoverageRatio* by hazard type and JPWI quartile.

Hazard-Zone Type	JPWI Quartile	Retained Cells	Included Cells, *n* (%) (*HazardInclusion* = 1)		*HazardCoverageRatio* Median	IQR	P95
Flood inundation zones	Q1	23,226	4409	(19.0%)	0.274	0.591	1.000
	Q2	27,030	9488	(35.1%)	0.616	0.744	1.000
	Q3	27,787	10,858	(39.1%)	0.775	0.635	1.000
	Q4	28,187	9933	(35.2%)	0.870	0.550	1.000
Storm surge inundation zones	Q1	23,226	409	(1.8%)	0.391	0.627	0.994
	Q2	27,030	1690	(6.3%)	0.806	0.608	1.000
	Q3	27,787	3147	(11.3%)	0.927	0.437	1.000
	Q4	28,187	5377	(19.1%)	0.984	0.265	1.000
Tsunami inundation zones	Q1	23,226	2013	(8.7%)	0.231	0.433	0.993
	Q2	27,030	3053	(11.3%)	0.496	0.734	1.000
	Q3	27,787	3699	(13.3%)	0.666	0.762	1.000
	Q4	28,187	3939	(14.0%)	0.871	0.605	1.000
Landslide warning zones	Q1	23,226	15,023	(64.7%)	0.404	0.463	0.931
	Q2	27,030	9643	(35.7%)	0.238	0.450	0.916
	Q3	27,787	6091	(21.9%)	0.148	0.329	0.827
	Q4	28,187	3356	(11.9%)	0.090	0.216	0.690

Note: Retained cells indicate the number of population core cells included in the analysis after excluding records affected by confidentiality-related suppression. Included cells indicate the number and percentage of population core cells with *HazardInclusion* = 1. Percentages were calculated using the retained cells in each JPWI quartile as the denominator. These percentages represent identified overlap in the available official hazard-zone layers and should not be interpreted as complete estimates of hazard presence or absence. The median, IQR, and P95 of *HazardCoverageRatio* were calculated among included cells for each hazard type and JPWI quartile. IQR indicates the interquartile range, and P95 indicates the 95th percentile.

3.2.2. Spatial Co-Distribution of Areal Overlap (Bivariate Maps)

Figures 6 and 7 illustrate bivariate maps showing the spatial co-distribution between JPWI categories and *HazardCoverageRatio* for flood inundation and landslide warning zones in the Tokyo metropolitan area. Light gray cells indicate population core cells for which no hazard-positive pixels were identified in the corresponding available hazard-zone layer. For flood inundation, population core cells with high JPWI (Q4) include both low and high *HazardCoverageRatio* categories, indicating heterogeneous spatial overlap. High-coverage cells in the Q4 *HazardCoverageRatio* category are particularly concentrated in major urban areas along Tokyo Bay, as well as in the downstream areas of major rivers such as the Arakawa, Edogawa, and Tamagawa. These patterns indicate that population core cells in these regions show relatively greater overlap with flood inundation zones. For landslide warning zones, high-coverage cells in the Q4 *HazardCoverageRatio* category are more frequently associated with low-JPWI population core cells (Q1). This pattern suggests that population core cells in lower JPWI strata within the mapped area tended to have more extensive overlap with designated landslide warning zones.

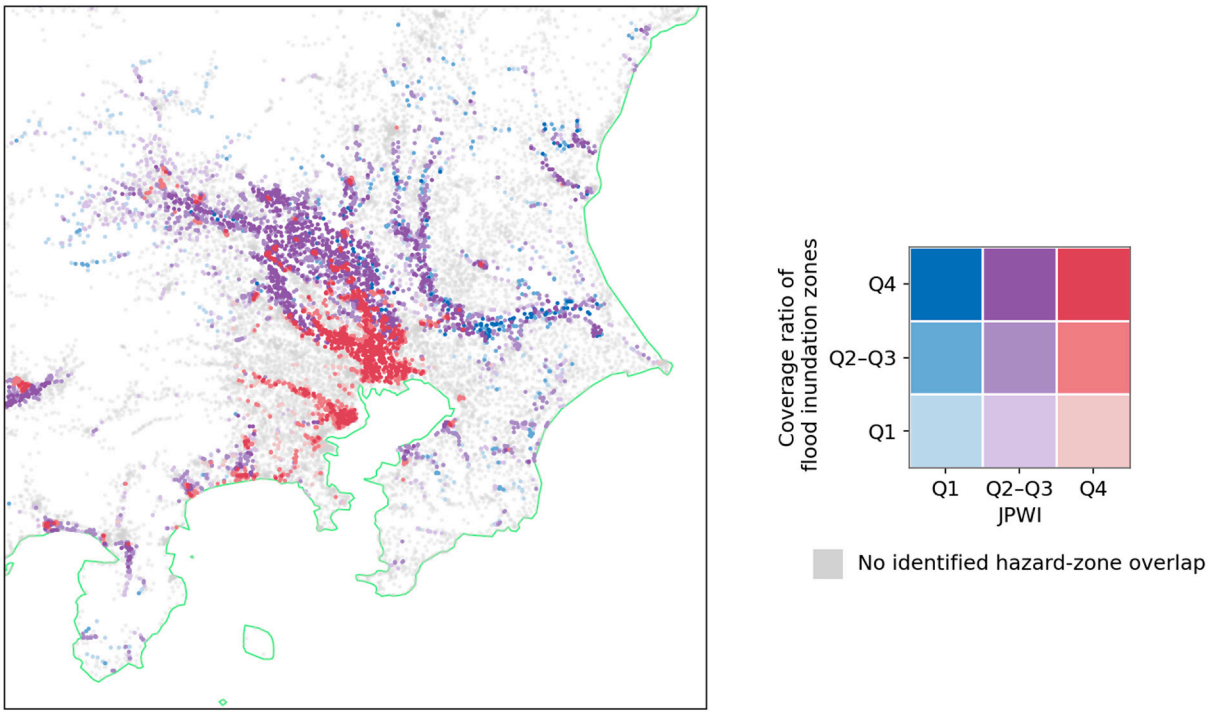


Figure 6. Bivariate classification map of population core cells by JPWI categories and *HazardCoverageRatio* for flood inundation in the Tokyo metropolitan area. Green lines indicate coastlines (land–sea boundaries) used as geographic reference.

3.3. Estimated Exposed Population by JPWI Quartiles

3.3.1. Distribution of Estimated Exposed Population (Boxplots)

Figure 8 shows the distribution of *HazardExposedPopulation* for each hazard type, stratified by JPWI quartiles. The number of included cells and descriptive statistics are reported in Table 5. Across the four hazard types, the median values of *HazardExposed-Population* tend to increase with JPWI quartile and are highest in Q4 among population core cells with *HazardInclusion* = 1. This pattern suggests that population core cells with identified hazard-zone overlap in higher JPWI quartiles tended to have larger estimated exposed populations. Because the estimated exposed population indicator incorporates cell population, these differences should be interpreted descriptively and in relation to the *HazardCoverageRatio* results.

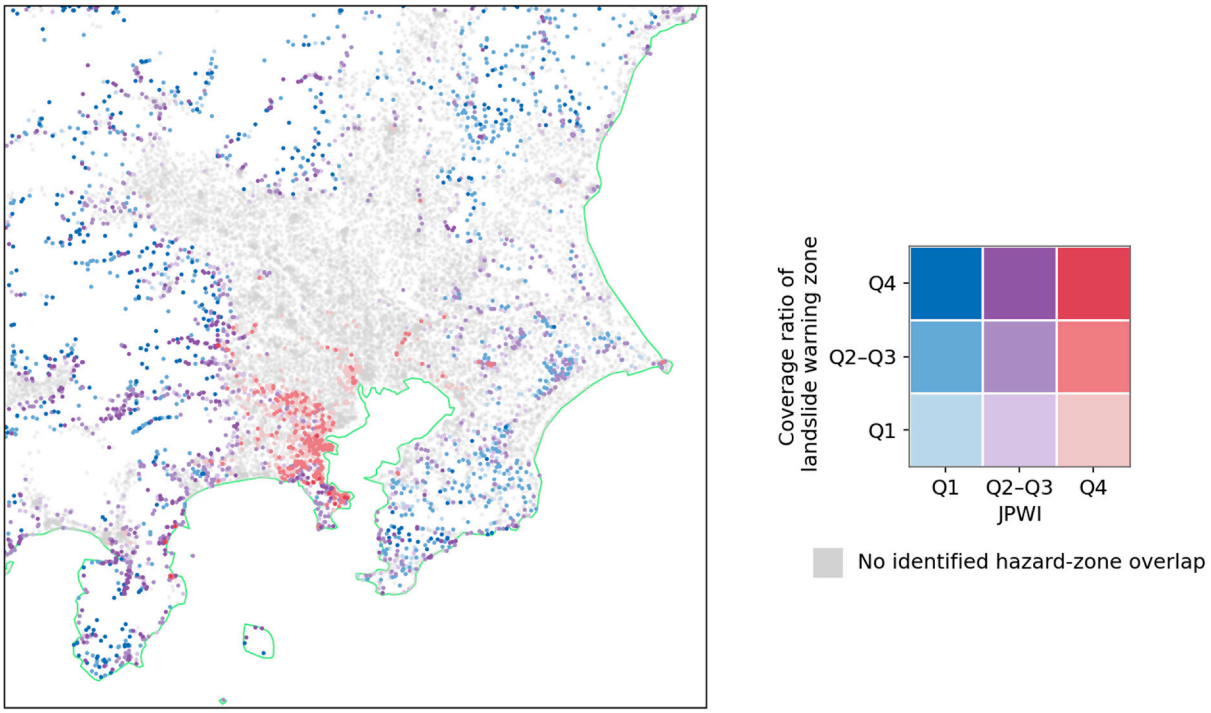


Figure 7. Bivariate classification map of population core cells by JPWI categories and *HazardCoverageRatio* for landslide warning zones in the Tokyo metropolitan area. Green lines indicate coastlines (land–sea boundaries) used as geographic reference.

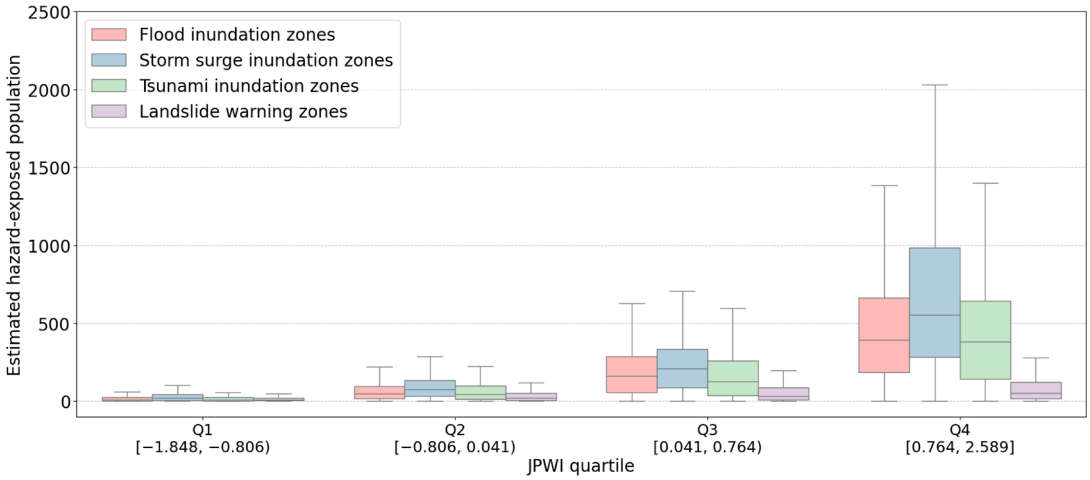


Figure 8. Distribution of estimated *HazardExposedPopulation* by JPWI quartile among population core cells with *HazardInclusion* = 1. Outliers are not shown for readability. Descriptive statistics are reported in Table 5.

3.3.2. Spatial Co-Distribution of Estimated Exposed Population (Bivariate Maps)

Figures 9 and 10 present bivariate maps showing the spatial co-distribution between JPWI categories and *HazardExposedPopulation* for flood inundation and landslide warning zones in the Tokyo metropolitan area. Light-gray cells indicate population core cells for which no hazard-positive pixels were identified in the corresponding available hazard-zone layer. For flood inundation zones, high-JPWI population core cells (Q4) frequently fall into categories with large *HazardExposedPopulation*, particularly in central and densely populated parts of the metropolitan area. For landslide warning zones, population core cells with high *HazardExposedPopulation* (Q4) appear across multiple JPWI categories, although their overall distribution is more scattered.

Table 5. Descriptive statistics of estimated *HazardExposedPopulation* by hazard type and JPWI quartile.

Hazard-Zone Type	JPWI Quartile	Retained Cells	Included Cells, *n* (%) (*HazardInclusion* = 1)		*HazardExposedPopulation*		
					Median	IQR	P95
Flood inundation zones	Q1	23,226	4409	(19.0%)	10.1	23.7	68.3
	Q2	27,030	9488	(35.1%)	47.4	81.7	207.9
	Q3	27,787	10,858	(39.1%)	160.3	229.4	489.0
	Q4	28,187	9933	(35.2%)	394.0	479.9	1487.6
Storm surge inundation zones	Q1	23,226	409	(1.8%)	19.8	39.0	96.9
	Q2	27,030	1690	(6.3%)	75.8	101.4	264.0
	Q3	27,787	3147	(11.3%)	210.0	248.3	561.0
	Q4	28,187	5377	(19.1%)	554.0	701.7	1967.0
Tsunami inundation zones	Q1	23,226	2013	(8.7%)	8.7	21.6	69.0
	Q2	27,030	3053	(11.3%)	44.5	85.2	207.6
	Q3	27,787	3699	(13.3%)	125.9	225.6	472.1
	Q4	28,187	3939	(14.0%)	382.4	503.7	1529.9
Landslide warning zones	Q1	23,226	15,023	(64.7%)	10.8	18.0	54.1
	Q2	27,030	9643	(35.7%)	20.7	44.3	129.7
	Q3	27,787	6091	(21.9%)	32.8	75.5	258.1
	Q4	28,187	3356	(11.9%)	51.3	105.9	389.8

Note: Retained cells indicate the number of population core cells included in the analysis after excluding records affected by confidentiality-related suppression. Included cells indicate the number of population core cells with *HazardInclusion* = 1. Percentages were calculated using the retained cells in each JPWI quartile as the denominator. These percentages represent identified overlap in the available official hazard-zone layers and should not be interpreted as complete estimates of hazard presence or absence. Median, IQR, and P95 were calculated for *HazardExposedPopulation* among included cells for each hazard type and JPWI quartile. IQR indicates the interquartile range, and P95 indicates the 95th percentile. Values of *HazardExposedPopulation* are expressed in persons.

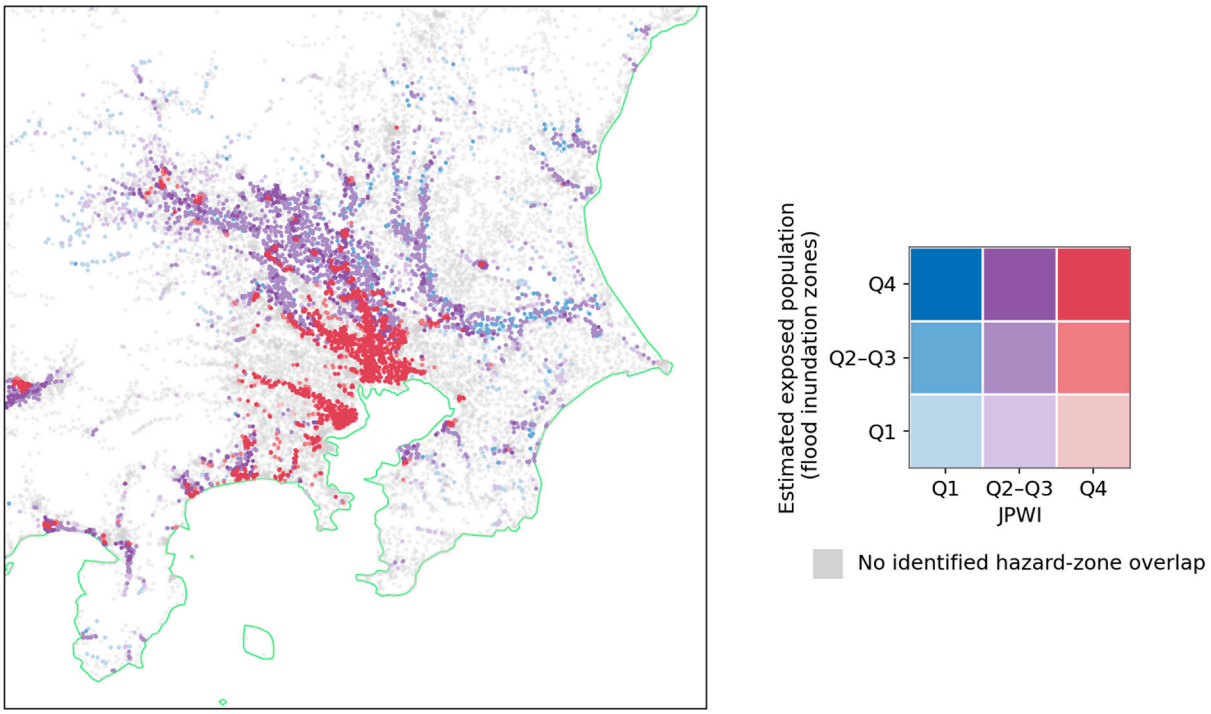


Figure 9. Bivariate map of JPWI categories and *HazardExposedPopulation* for flood inundation zones among postcode-level population core cells in the Tokyo metropolitan area. Green lines indicate coastlines (land–sea boundaries) used as geographic reference.

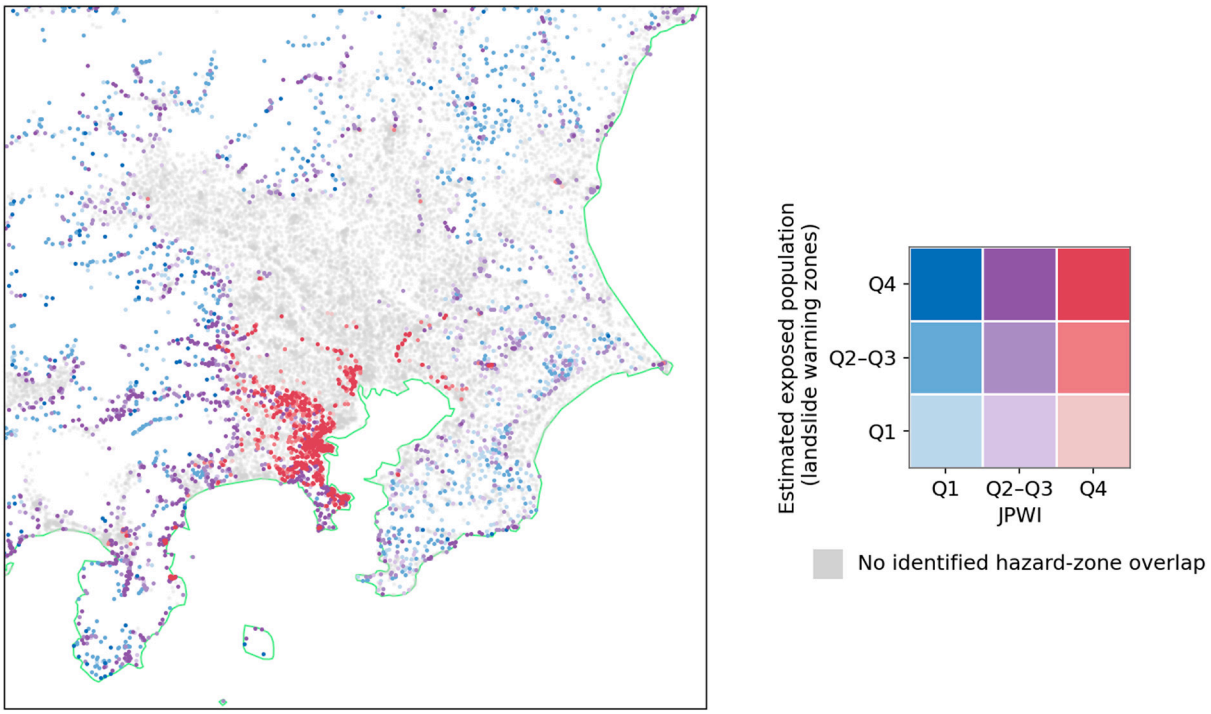


Figure 10. Bivariate map of JPWI categories and *HazardExposedPopulation* for landslide warning zones among postcode-level population core cells in the Tokyo metropolitan area. Green lines indicate coastlines (land–sea boundaries) used as geographic reference.

3.4. Overview of Key Results and Supplementary Analyses

As summarized in Figures 4, 5 and 8, and Tables 4 and 5, *HazardInclusion*, *HazardCoverageRatio*, and *HazardExposedPopulation* showed different patterns across JPWI quartiles by hazard type. Population core cells in high-JPWI strata overlapped more frequently with flood, storm surge, and tsunami inundation zones, whereas population core cells in low-JPWI strata overlapped more frequently with designated landslide warning zones. In addition, among population core cells where spatial overlap with hazard zones was identified, estimated exposed populations tended to be larger in high-JPWI strata across all hazard types. However, *HazardInclusion* results should be interpreted as identified overlap in the available hazard-zone layers and not as complete estimates of hazard presence or absence. In addition, the larger estimated exposed populations observed in high-JPWI strata should be interpreted as descriptive results and not as evidence that walkability itself independently explains larger exposed populations.

As a supplementary diagnostic comparison, Appendix C, Table A2 compares hazard-zone indicators calculated using postcode-level population core-cell records with those calculated using all populated 250 m census grid cells in selected case-study regions. The comparison showed that the two spatial representations produced generally comparable but not identical values, with differences varying by hazard type. These results indicate that the population core-cell approach should not be interpreted as equivalent to an all-populated-cell representation of broader local areas.

As a supplementary local-neighborhood sensitivity analysis, we examined whether the JPWI-stratified patterns observed in the main core-cell analysis were sensitive to the use of only the representative population core cell (Appendix D, Table A3). The 3 × 3-neighborhood results showed patterns broadly consistent with the main core-cell analysis. *HazardInclusion* proportions were similar to the main core-cell proportions, and although *HazardCoverageRatio* values were lower in absolute terms, the JPWI-stratified

tendencies were consistent with the main results. The mean 3 × 3-neighborhood sums of *HazardExposedPopulation* also showed patterns consistent with the main findings.

The combinations of identified hazard-zone types within the same population core cells were further summarized in Appendix E. Most population core cells had zero or one identified hazard-zone type, while cells with three or four identified hazard-zone types were relatively uncommon. These counts should not be interpreted as simultaneous or compound hazard events, cumulative exposure, or compound risk.

4. Discussion

This section discusses the descriptive national-scale patterns of hazard-zone overlap and estimated exposed population identified in Section 3, derived using the nationally consistent analytical framework developed in this study. The focus is on differences across walkability-based urban spatial characteristics represented by JPWI strata. The discussion remains descriptive rather than causal, because the primary purpose of this study is to establish a nationally consistent basis for characterizing hazard-zone-based estimated population exposure across JPWI-defined urban spatial contexts in Japan.

4.1. JPWI and Hazard-Zone Overlap

For flood, storm surge, and tsunami inundation zones, Q2–Q4 generally showed higher proportions of population core cells with *HazardInclusion* = 1 than Q1, along with larger median and upper-quantile values of areal overlap within included cells (*HazardCoverageRatio*). In contrast, for landslide warning zones, lower JPWI quartiles showed higher inclusion proportions, and *HazardCoverageRatio* values were also larger. These tendencies were also reflected in the bivariate maps presented in Section 3.2.2 (Figures 6 and 7), with corresponding national maps provided in Appendix B. These results indicate systematic differences in identified hazard-zone overlap across JPWI strata at the national scale, with contrasting tendencies across hazard types. The storm surge and tsunami inundation zones analyzed in this study are geographically concentrated in coastal areas. Therefore, the higher inclusion proportions in high-JPWI strata may partly reflect the concentration of high-JPWI population core cells in coastal urban areas.

These patterns should not be interpreted as evidence that JPWI independently explains hazard-zone overlap or estimated exposed population. The analysis did not adjust for topography, coastal location, land use, or other geographic factors. Instead, the observed JPWI-stratified patterns likely reflect the spatial co-distribution of JPWI-defined urban spatial contexts with Japan's broader settlement geography, including dense coastal lowlands and metropolitan areas as well as rural, hilly, or mountainous settlements. In this sense, the results should be understood as descriptive co-distribution patterns, rather than as evidence of an independent or causal effect of JPWI on hazard-zone overlap or estimated exposed population. Although this study does not identify the mechanisms underlying these co-distribution patterns, it documents where JPWI-stratified differences are observed and for which hazard types they are most evident. These descriptive findings may serve as a starting point for future studies examining whether topography, coastal location, land-use context, and the individual components of JPWI partly account for the observed JPWI-stratified differences.

The supplementary case-study comparison in Appendix C, Table A2, which used all populated 250 m census grid cells in selected regions, further supports this cautious interpretation. In the selected regions, the population core-cell representation and the all-populated-cell representation produced broadly related but not equivalent values, with differences varying by hazard type. Core-cell values tended to be higher for several inundation-related indicators, whereas all-cell values tended to be higher for landslide

warning-zone overlap. These results indicate that population core cells characterize representative population concentrations associated with postcode areas but do not necessarily represent all populated locations in broader local areas. Accordingly, the JPWI-stratified results should be interpreted as descriptive patterns at postcode-level population core cells, not as complete local-area or whole-postcode exposure estimates.

4.2. Exposed Population at Population Core Cells

Section 3.3 showed that estimated exposed populations among included cells differed across JPWI quartiles in both magnitude (Figure 8) and spatial pattern (Figures 9 and 10). For flood, storm surge, and tsunami inundation zones, higher JPWI quartiles tended to have larger estimated exposed populations when spatial overlap with hazard zones was identified. This pattern is partly expected because the exposed population estimate incorporates cell population, and JPWI includes a population-density component. However, these population-related quantities are not calculated over the same spatial unit. The exposed population estimate is based on the 250 m population core cell, whereas the JPWI population-density component is based on the 1 km network-based walking catchment from each postcode representative point. For landslide warning zones, the results should be interpreted together with the inclusion and coverage patterns. In lower JPWI quartiles, core cells were more frequently included in landslide warning zones and tended to have larger areal coverage, but their populations were generally smaller. In higher JPWI quartiles, overlap with landslide warning zones was less frequent, but when it occurred, larger core-cell populations could result in greater estimated exposed populations.

Because *HazardExposedPopulation* is calculated by multiplying *HazardCoverageRatio* by the population of each core cell, variation in this indicator reflects both the areal coverage of hazard zones and the population size of the cell. By reporting *HazardCoverageRatio* separately from *HazardExposedPopulation*, this study helps distinguish, at a descriptive level, the areal-overlap component of exposure from the cell-population component. In addition, because JPWI includes population density as one of its components, the larger estimated exposed populations observed in high-JPWI strata should not be interpreted as evidence of an independent effect of walkability-related urban characteristics. Rather, they may partly reflect the population-density component of JPWI and the concentration of dense settlements, particularly in lowland, coastal, and metropolitan areas.

The JPWI component variables summarized in Appendix A, Table A1, were calculated within the 1 km network-based walking catchment around each postcode representative point, whereas *HazardExposedPopulation* was calculated at the 250 m population core-cell level. Therefore, the component-level summary should be interpreted as a diagnostic aid for understanding the population-density component of JPWI, not as a population-adjusted analysis or a component-level causal assessment.

4.3. Implications for Disaster Preparedness

The JPWI-stratified results provide screening-level baseline information for framing disaster-preparedness planning questions across different JPWI-defined urban spatial characteristics and hazard-zone-based exposure patterns. These findings are intended to support planning and review processes, such as revisions of local disaster management and evacuation plans, rather than to prescribe specific countermeasures. For forecast- or warning-based hazards, including flood inundation, storm surge, tsunami inundation, and landslide-related hazards represented by designated landslide warning zones, the results may help local governments identify aspects of existing evacuation planning that require review, including evacuation-center capacity, evacuation modes, route guidance, and communication arrangements [8,28]. These planning implications are consistent with

Priority 4 of the Sendai Framework, which emphasizes enhancing disaster preparedness for effective response. However, the choice of concrete measures should depend on local conditions and detailed hazard assessments by each local government.

For high-JPWI population core cells overlapping with inundation-related hazard zones, including flood, storm surge, and tsunami inundation zones, the results suggest that further review may be warranted regarding the adequacy of evacuation information, route guidance, signage, assembly points, evacuation sites, and evacuation-center capacity, particularly where estimated exposed populations are large [8,28–30]. In particular, where high-JPWI core cells coincide with inundation zones, evacuation route information and guidance may require periodic review in terms of clarity, visibility, and practical usability [29,30]. These considerations are consistent with previous discussions on evacuation planning and the relationship between walkability and resilience [18,19,28–30].

For low-JPWI population core cells overlapping with designated landslide warning zones, the results suggest a different set of planning questions. Because these areas may include more rural, hilly, or less densely settled contexts, further review may be warranted regarding evacuation timing, possible isolation, mobility constraints, local communication arrangements, and the siting of evacuation facilities [28,31]. These issues are particularly relevant when considering staged pre-evacuation for rainfall-related hazards in landslide warning zones [28,31].

Overall, these findings provide a nationally consistent, screening-level baseline that may serve as a preliminary reference for reviewing disaster-preparedness planning. Because this study did not directly measure evacuation behavior, shelter accessibility, road capacity, travel time, age structure, disability, car ownership, road-network disruption, or other dimensions of population vulnerability, these implications should be interpreted as indirect planning considerations rather than direct policy conclusions.

4.4. Contributions of This Study

The main contributions of this study can be summarized in three points. First, this study provides a nationwide, walkability-stratified characterization of hazard-zone overlap and estimated exposed population for four hazard types examined separately, using postcode-level population core cells as a common spatial unit. By applying this common spatial unit, the study supports consistent interpretation of indicators derived from hazard-zone layers across JPWI strata for each hazard type within the stated methodological limitations. Prior walkability–hazard research has largely focused on region-specific analyses, such as studies of the Tokyo metropolitan area [20] or single-site case studies [21], limiting national-scale characterization based on a common spatial unit. This study extends prior work by providing a nationwide descriptive baseline within a unified analytical framework.

Second, this study presents a nationally consistent and reproducible analytical framework that integrates hazard-zone layers, JPWI as a nationwide walkability index, and population distribution. This framework supports systematic characterization of hazard-zone-based estimated population exposure across diverse urban spatial characteristics and provides a screening-level baseline for disaster-preparedness discussions. By building on openly available source data and archiving the final analysis subset for public release upon acceptance [27], this study also improves the reproducibility and reusability of the analysis.

Third, within this nationally consistent framework, the three descriptive indicators in Section 3, namely *HazardInclusion*, *HazardCoverageRatio*, and *HazardExposedPopulation*, showed that hazard-zone overlap and estimated exposed population vary across JPWI strata in a hazard-specific manner rather than following a uniform pattern across hazard types. Flood, storm surge, and tsunami inundation zones generally showed higher pro-

portions of cells with *HazardInclusion* = 1 in Q2–Q4 than in Q1, whereas landslide warning zones showed higher *HazardInclusion* proportions in low-JPWI quartiles. These contrasting tendencies indicate that patterns of hazard-zone overlap and hazard-zone-based estimated population exposure differ by hazard type across walkability-based urban spatial characteristics. Although the analysis is limited to postcode-level population core cells and does not estimate total hazard-zone-based exposure within entire postcode areas, it provides a common and nationally consistent baseline for characterizing how designated hazard-zone overlap and estimated exposed population are distributed across JPWI-defined urban spatial contexts in Japan.

4.5. Limitations and Future Research

First, the publicly available hazard data used in this study do not necessarily provide complete nationwide coverage. The analysis relies on published categorical hazard-zone layers, such as designated flood inundation zones and landslide warning zones, and on 250 m grid population data. In addition, hazard intensity measures, such as inundation depth for flood, storm surge, and tsunami, or distinctions between warning and special-warning classes for landslides, were not considered. Therefore, the estimated areal overlap and estimated exposed population should be interpreted as approximate representations of hazard-zone-based exposure patterns rather than precise measurements. This study analyzes overlap with designated hazard-zone layers and does not estimate hazard probability, expected event frequency, event likelihood, or expected loss. For landslide-related zones, the results should be interpreted as a broad characterization of overlap with designated landslide warning zones, not as an assessment of landslide hazard severity, special-warning status, or regulatory risk level. Because the source hazard-zone layers do not provide uniform nationwide coverage and explicit coverage masks were not consistently available, this study could not reliably distinguish cells outside effective hazard-data coverage from cells where no hazard-positive pixels were identified. Therefore, *HazardInclusion* proportions were calculated using retained population core cells as the denominator and should be interpreted as indicators of identified hazard-zone overlap in the available hazard-zone layers, not as complete estimates of hazard presence or confirmed absence.

Second, for each postcode area, we used the 250 m grid cell corresponding to the JPWI representative point as the "population core cell." This definition follows the JPWI framework, in which the representative point is the center coordinate of the most populous 250 m grid cell within a postcode area. Therefore, the results characterize hazard-zone overlap and estimated exposed population at postcode-level population core cells and should not be interpreted as estimates of total hazard-zone-based exposure within entire postcode areas or as detailed site-specific risk assessments. The supplementary 3 × 3-neighborhood sensitivity analysis in Appendix D provides a local-neighborhood robustness check, but it does not validate the method against whole-postcode exposure estimates. The supplementary case-study comparison in Appendix C further showed that core-cell-based indicators and all-populated-cell indicators were broadly related but not equivalent. Thus, the main findings should be interpreted as descriptive patterns at postcode-level population core cells, not as complete local-area or whole-postcode exposure estimates.

Although the case-study comparison in Appendix C included selected regions with different broad geographic contexts, this study did not conduct a formal nationwide stratification or adjustment by coastal versus inland, lowland versus mountainous, or metropolitan versus non-metropolitan settings. Therefore, the JPWI-stratified patterns may partly reflect geographic factors related to Japan's broader settlement geography and should not be interpreted as effects of JPWI-defined urban spatial characteristics alone. In addition, confidentiality-related suppression of census grid cells affected Q1 more strongly than the

other JPWI quartiles, and possible spatial concentration of excluded records remains a limitation. Future research should examine these issues using all populated 250 m cells within complete local administrative units and nationally consistent geographic stratifications.

Third, the relationships among JPWI, hazard-zone overlap, and estimated exposed population were analyzed using data from a single point in time; temporal change was not considered. Previous research [6] has shown that population and household numbers within designated flood inundation zones in Japan have increased since 1995, highlighting the importance of finer-scale analyses for understanding population dynamics in areas within designated hazard zones. Future research could examine the relationship between JPWI and population change from 2020 onward within designated flood inundation zones, with possible extension to other hazard zones in subsequent analyses.

Fourth, JPWI includes population density as one of its components, and population is also used to calculate *HazardExposedPopulation*. Therefore, the association between higher JPWI strata and larger estimated exposed populations should not be interpreted as an independent or causal effect of walkability-related urban characteristics. Rather, the results characterize hazard-zone-based exposure patterns within JPWI-defined urban spatial contexts, which reflect the combined influence of population density, facility diversity, and street connectivity. By reporting *HazardCoverageRatio* separately from *HazardExposedPopulation*, this study helps distinguish, at a descriptive level, the areal-overlap component from the cell-population component of estimated exposure. However, this separation does not identify the independent effects of individual JPWI components. This study did not include land use, elevation, slope, distance to coastline, municipality type, or other geographic factors that may confound the relationship between JPWI strata and hazard-zone overlap. In addition, the component-level effects of JPWI, including population density, facility diversity, and street connectivity, were not estimated separately. Such adjusted or component-level analyses would require additional datasets and a different modeling framework and are therefore left for future research.

Building on these limitations, future research should incorporate hazard intensity measures, analyses using all populated grid cells or entire postcode areas, temporal population change, geographic covariates, and component-level analyses of JPWI. Such extensions would support a more nuanced characterization of hazard-zone-based exposure patterns across hazard types and urban spatial contexts.

5. Conclusions

This study developed a nationally consistent descriptive framework for characterizing hazard-zone-based estimated population exposure for four hazard types across JPWI-defined urban spatial contexts in Japan. The analysis was conducted at postcode-level population core cells and was not designed to estimate total hazard-zone-based exposure within entire postcode areas. The hazard-zone layers were analyzed separately by hazard type; therefore, the findings should not be interpreted as a complete assessment of simultaneous or compound hazard events, cumulative exposure, or compound risk. In addition, the analysis was based on overlap with designated hazard-zone layers and did not estimate hazard probability, expected event frequency, event likelihood, or expected loss.

By using postcode-level population core cells as a common spatial unit, the analysis supported consistent characterization of hazard-zone inclusion, areal overlap, and estimated exposed population. The results show that higher-JPWI strata generally had more frequent overlap with flood, storm surge, and tsunami inundation zones than Q1, whereas low-JPWI population core cells more often overlapped with designated landslide warning zones. Where hazard-zone overlap was identified, estimated exposed populations tended to be larger in high-JPWI strata. However, this pattern should be interpreted descrip-

tively because the exposure estimate incorporates cell population and JPWI includes a population-density component. It should not be interpreted as an independent effect of walkability itself.

Overall, the findings indicate that hazard-zone overlap and hazard-zone-based estimated exposed population show consistent differences across JPWI strata at the national scale in Japan, and that these patterns differ by hazard type. Because the analysis is based on postcode-level population core cells and available hazard-zone data, the findings should be interpreted as a national-scale characterization of exposure patterns rather than as estimates of total hazard-zone-based exposure within entire postcode areas or as detailed local risk assessments. Within these methodological constraints, this study provides a nationally consistent descriptive baseline for characterizing designated hazard-zone overlap and estimated exposed population at postcode-level population core cells in Japan. Future research should extend this framework by incorporating analyses based on all populated grid cells or entire postcode areas, hazard intensity measures, explicit hazard-data coverage information, topographic and coastal variables, land-use characteristics, demographic vulnerability, and evacuation-related indicators.

Author Contributions: Conceptualization, K.U. and O.U.; methodology, K.U.; validation, K.U. and O.U.; formal analysis, K.U.; investigation, K.U.; resources, K.U.; data curation, K.U.; writing—original draft preparation, K.U.; writing—review and editing, K.U. and O.U.; visualization, K.U.; supervision, O.U.; project administration, O.U.; funding acquisition, O.U. All authors have read and agreed to the published version of the manuscript.

Funding: This research was supported by an annual grant from the Tokai University Research and Information Center (TRIC) for the fiscal years 2025 and 2026.

Institutional Review Board Statement: Not applicable.

Informed Consent Statement: Not applicable.

Data Availability Statement: The source integrated dataset generated for this study, which integrates hazard layers from the GSI Hazard Map Portal with the 2020 Population Census 250 m grid, is publicly available on Zenodo: https://doi.org/10.5281/zenodo.19230374. Hazard information was obtained from the GSI Hazard Map Open Data Portal: https://disaportal.gsi.go.jp/hazardmapportal/hazardmap/copyright/opendata.html (accessed on 31 January 2026). The 250 m population grid data from the 2020 Population Census were obtained from the Portal Site of Official Statistics of Japan (e-Stat): https://www.e-stat.go.jp/gis/statmap-search?page=1&type=1&toukeiCode=00200521&toukeiYear=2020&aggregateUnit=H&serveyId=H002005112020&statsId=T001141&datum=2011 (accessed on 31 January 2026). The Japan Postcode-level Walkability Index (JPWI), used for stratification, was obtained from [16] and is available as Version 2 on J-STAGE Data (https://jstagedata.jst.go.jp/articles/dataset/Japan_Postcode-level_Walkability_Index_JPWI_/22597090) (accessed on 1 February 2026). The final analysis subset used in this study was derived from the source integrated 250 m grid dataset by restricting the data to postcode-level population core cells consistent with the JPWI definition. It is publicly available on Zenodo (DOI: 10.5281/zenodo.19313406) (accessed on 18 May 2026).

Acknowledgments: During the preparation of this manuscript, the authors used Google Gemini (Gemini 3 Flash; Google LLC) to assist with generating and revising code for data analysis and figure preparation. ChatGPT (GPT-5.5 Thinking; OpenAI, San Francisco, CA, USA; used in March–June 2026) and Microsoft 365 Copilot (Think Deeper mode; Microsoft Corporation, Redmond, WA, USA; used in March–June 2026) were used to support AI-assisted language checking and wording refinement. The authors reviewed, edited, and verified all AI-assisted outputs, including generated code, edited text, and figure-preparation materials. Generated code was executed and checked by the authors. The authors take full responsibility for the content of this publication.

Conflicts of Interest: The authors declare no conflicts of interest.

Appendix A. National Distribution and Component-Level Summary of JPWI

Figure A1 provides the national distribution of JPWI quartiles at postcode-level population core cells, complementing the Tokyo metropolitan area map shown in Figure 3. Table A1 summarizes the JPWI component variables by JPWI quartile for the retained postcode-level population core-cell records. These component variables were calculated within the 1 km network-based walking catchment around each postcode representative point and should not be interpreted as measurements within the 250 m population core cell itself.

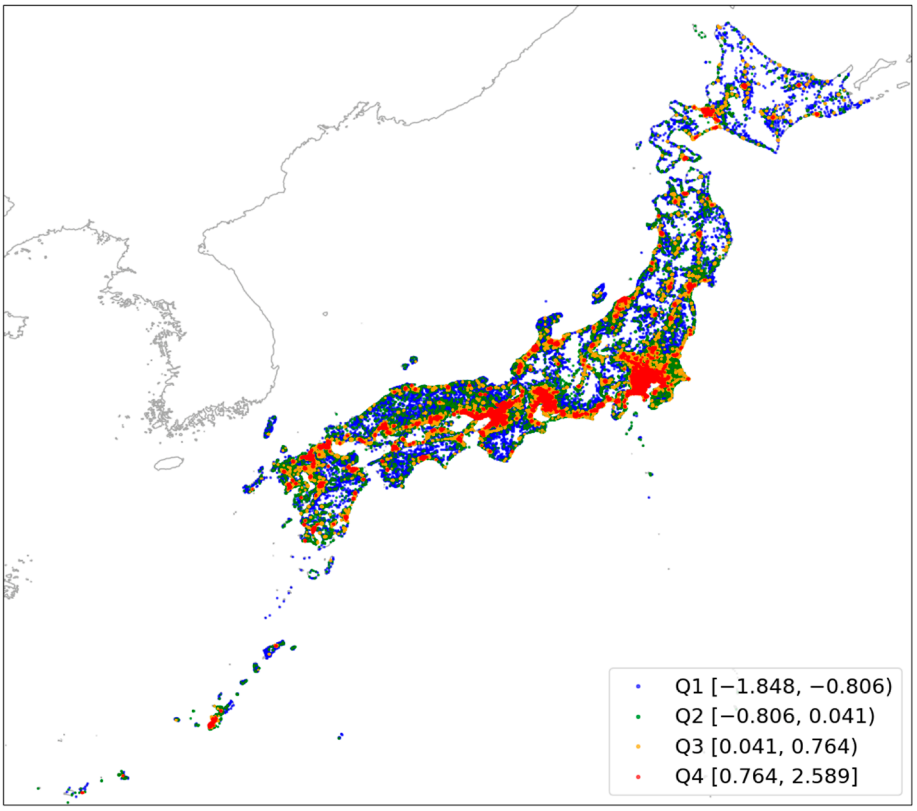


Figure A1. National distribution of JPWI quartiles at postcode-level population core cells.

Table A1. Supplementary component-level summary of JPWI by quartile.

JPWI Quartile	Retained Core-Cell Records, *n*	Population Density		Intersection Density		Facility-Type Diversity	
		Median	IQR	Median	IQR	Median	IQR
Q1	23,226	257.1	212.3	16.3	16.5	1	2
Q2	27,030	800.0	597.3	60.1	38.2	6	4
Q3	27,787	2819.1	1518.5	137.1	47.3	13	4
Q4	28,187	7741.2	5822.9	222.6	67.6	16	2

Note: Values are summarized for retained postcode-level population core-cell records. Population density, intersection density, and facility-type diversity are component variables of JPWI and were calculated within the 1 km network-based walking catchment around each postcode representative point, not within the 250 m population core cell itself. This table was prepared as a supplementary diagnostic summary to support interpretation of the relationship between JPWI and *HazardExposedPopulation* and is not intended to estimate the independent effect of each JPWI component on *HazardExposedPopulation*.

Appendix B. National Bivariate Maps

This appendix provides nationwide maps that correspond to the JPWI-stratified hazard analyses presented in the main text. For each hazard type, the figures visualize the spatial distribution of bivariate categories based on JPWI and either *HazardCoverageRatio*

or *HazardExposedPopulation* at population core cells. These maps serve as supplementary materials to complement the regional examples shown in the main text and allow readers to view the JPWI-stratified results at a nationwide scale.

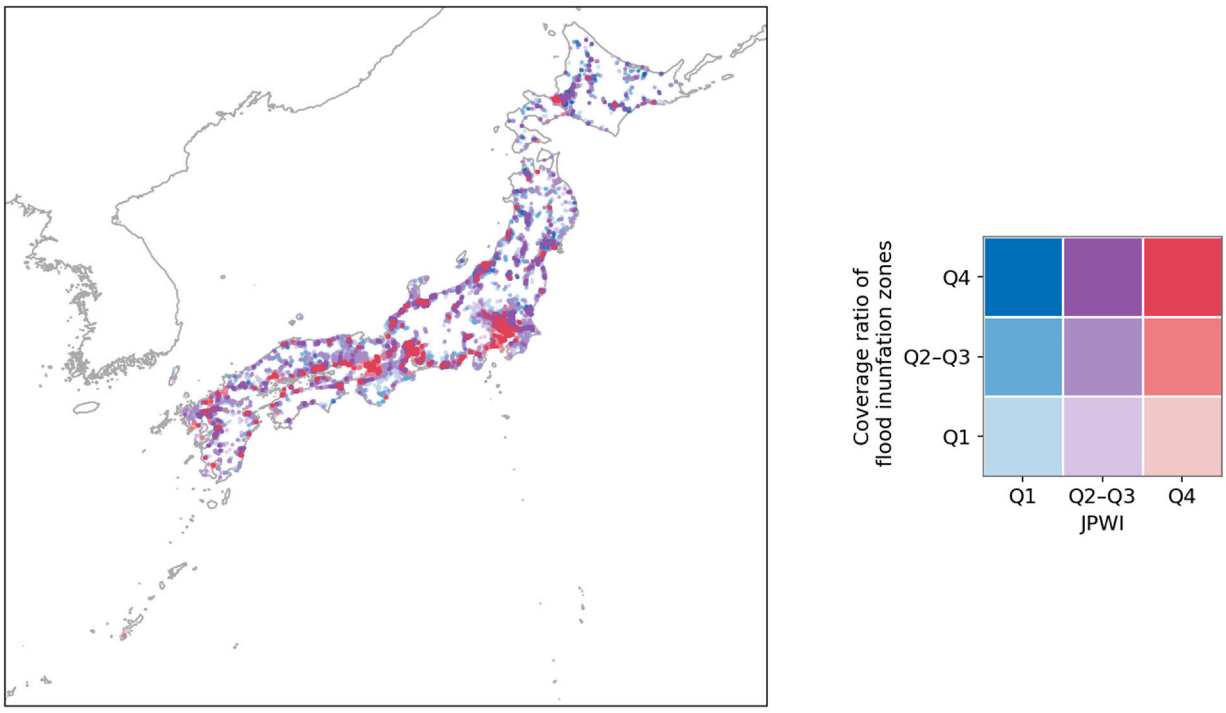


Figure A2. National bivariate map of JPWI categories and coverage ratio of flood inundation zones among postcode-level population core cells with identified hazard-zone overlap.

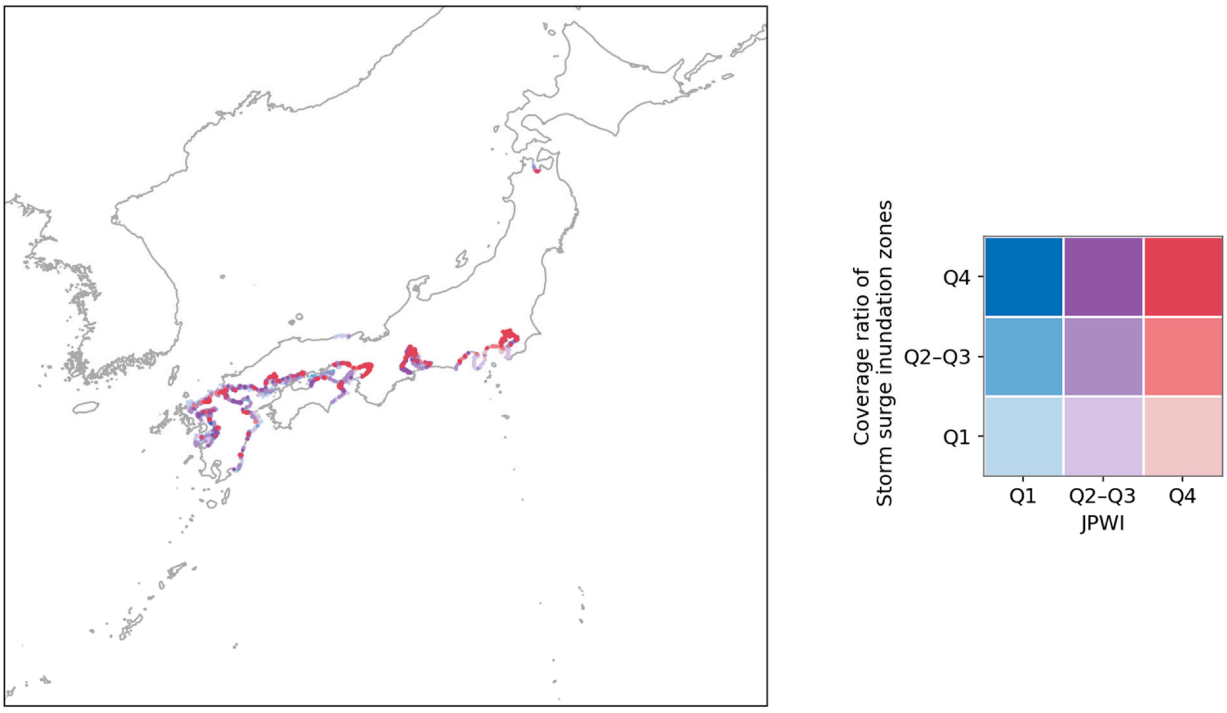


Figure A3. National bivariate map of JPWI categories and coverage ratio of storm surge inundation zones among postcode-level population core cells with identified hazard-zone overlap.

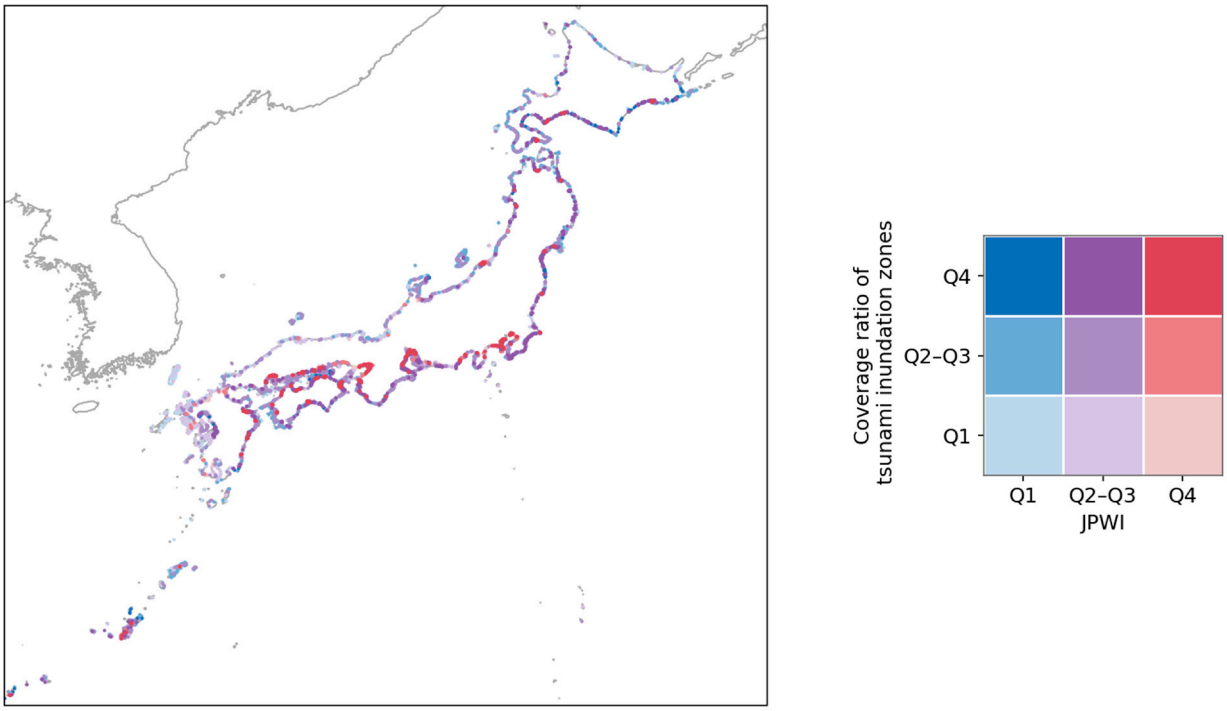


Figure A4. National bivariate map of JPWI categories and coverage ratio of tsunami inundation zones among postcode-level population core cells with identified hazard-zone overlap.

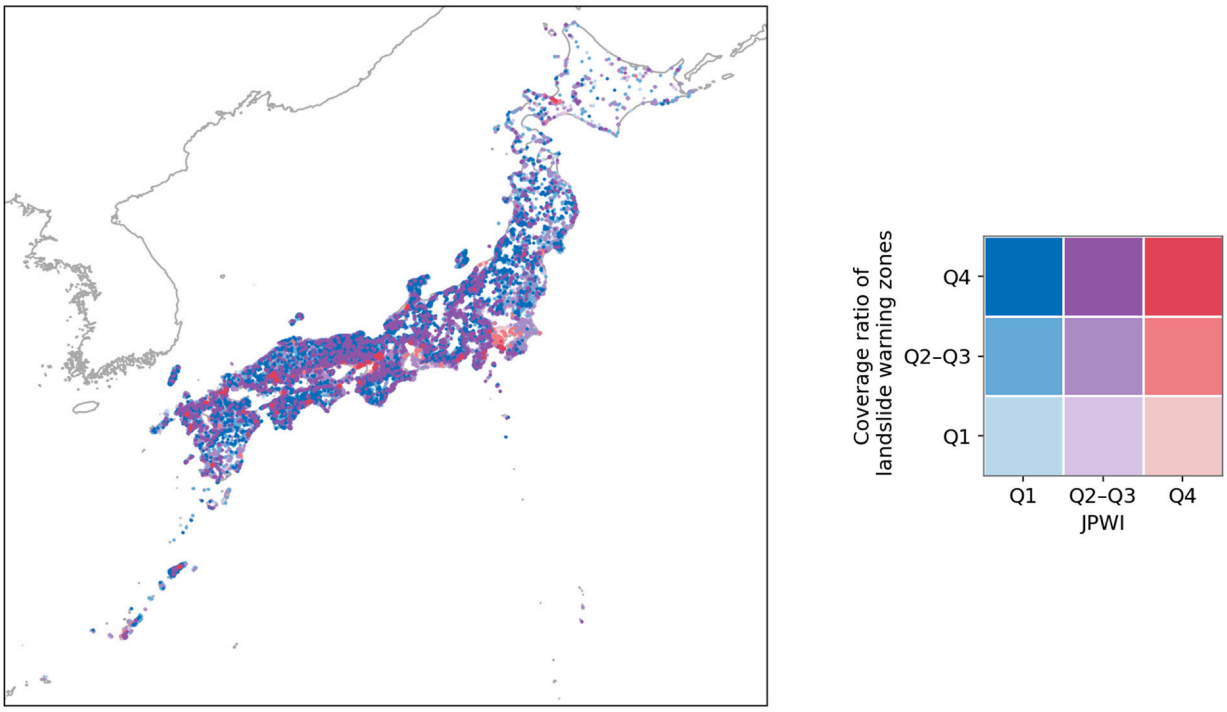


Figure A5. National bivariate map of JPWI categories and coverage ratio of designated landslide warning zones among postcode-level population core cells with identified hazard-zone overlap.

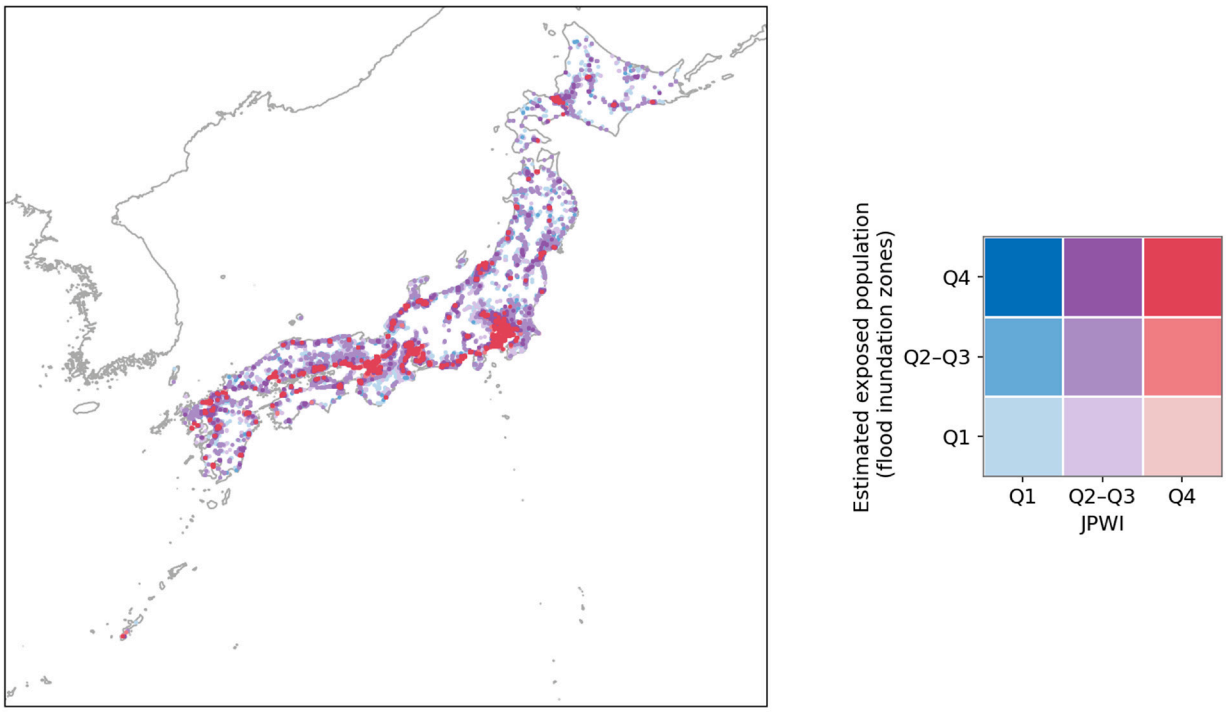


Figure A6. National bivariate map of JPWI categories and estimated exposed population for flood inundation zones among postcode-level population core cells with identified hazard-zone overlap.

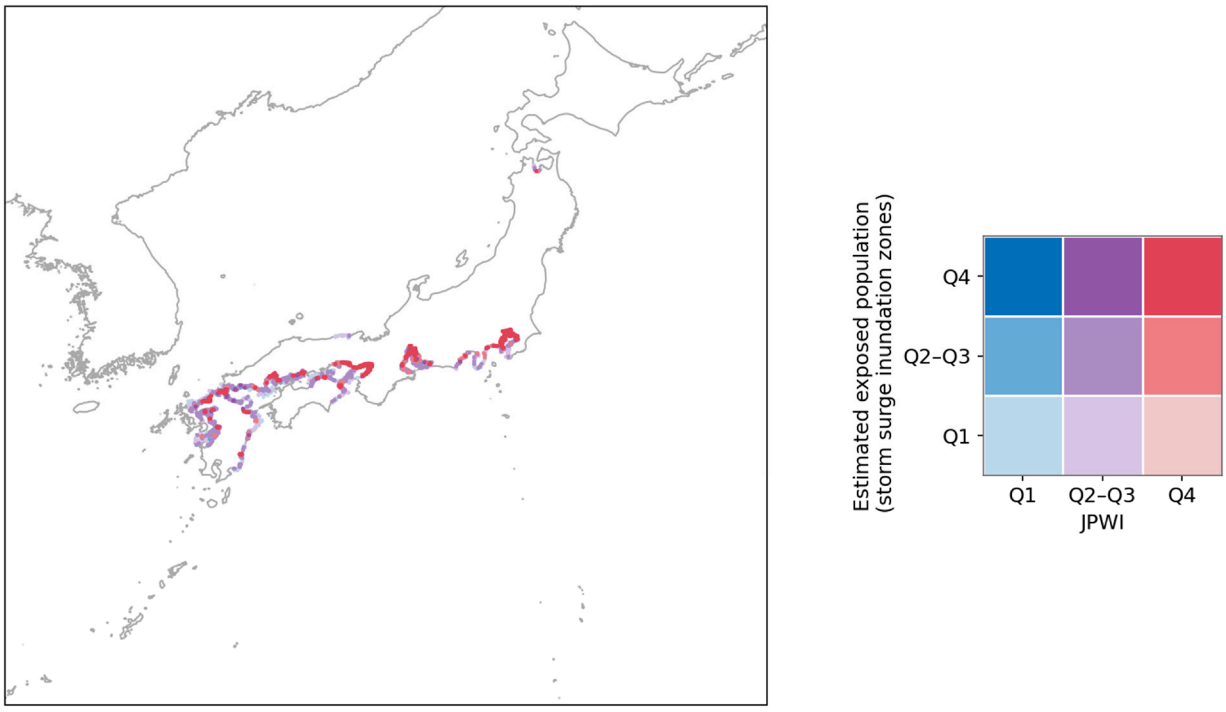


Figure A7. National bivariate map of JPWI categories and estimated exposed population for storm surge inundation zones among postcode-level population core cells with identified hazard-zone overlap.

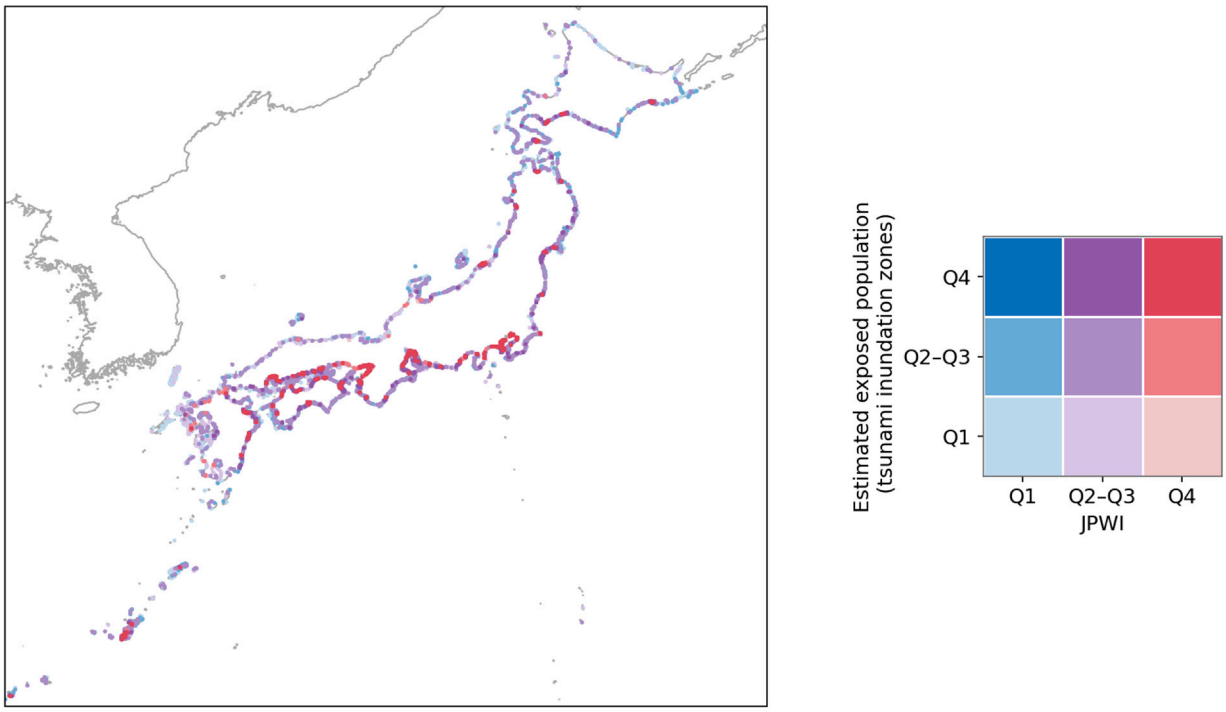


Figure A8. National bivariate map of JPWI categories and estimated exposed population for tsunami inundation zones among postcode-level population core cells with identified hazard-zone overlap.

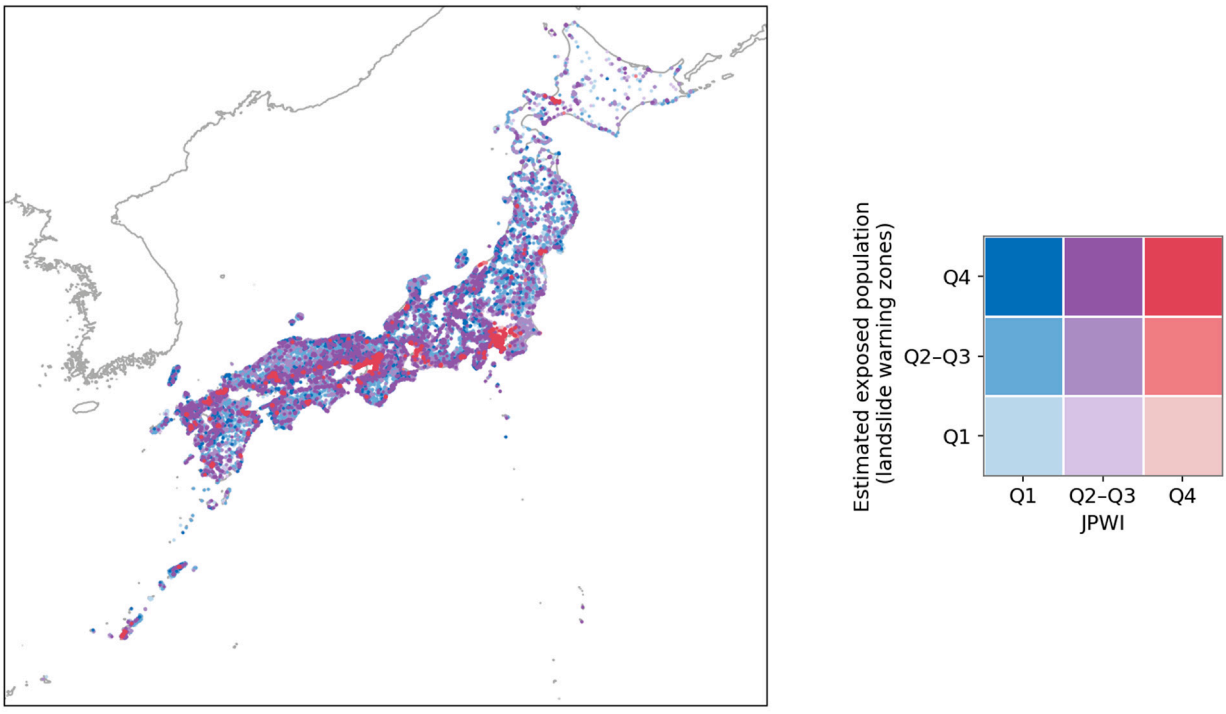


Figure A9. National bivariate map of JPWI categories and estimated exposed population for designated landslide warning zones among postcode-level population core cells with identified hazard-zone overlap.

Appendix C. Supplementary Case-Study Comparison Using All Populated 250 m Census Grid Cells

The selected case-study regions were Tokyo Metropolis, Osaka Prefecture, Shizuoka Prefecture, and Nagano Prefecture. These regions were selected to provide a supplementary diagnostic comparison across different broad geographic contexts. Tokyo Metropolis

and Osaka Prefecture were used as examples of metropolitan coastal contexts, Shizuoka Prefecture as an example of a coastal and mountainous context, and Nagano Prefecture as an example of an inland mountainous context. Tokyo Metropolis was treated as a prefecture-level administrative unit and therefore includes its island municipalities. For each selected region and hazard type, hazard-zone indicators were calculated separately for postcode-level population core-cell records and for all populated 250 m census grid cells in the region. We summarized the number of analysis units, the proportion of units with *HazardInclusion* = 1, mean *HazardCoverageRatio*, and mean *HazardExposedPopulation* per analysis unit. JPWI quartiles were not assigned to all populated 250 m census grid cells because JPWI is defined for postcode representative points and their 1 km network-based walking catchments, not for all populated cells. Therefore, this comparison should be interpreted as a diagnostic check of spatial representation rather than as a replacement for the nationwide postcode-level population core-cell analysis.

Table A2. Supplementary case-study comparison between postcode-level population core-cell records and all populated 250 m census grid cells in selected regions.

Case-Study Region	No. of Analysis Units, *n*		Hazard Type	Proportion of Cells with *HazardInclusion* = 1			Mean *HazardCoverageRatio*		Mean *HazardExposedPopulation*, Persons per Cell	
	Core-Cell Records	All Populated Cells		Core-Cell	All Populated Cells	Diff. (All-Core)	Core-Cell	All Populated Cells	Core-Cell	All Populated Cells
Tokyo Metropolis	1650	17,542	Flood	0.310	0.285	−0.024	0.231	0.201	389.4	221.3
			Storm surge	0.241	0.194	−0.047	0.183	0.151	340.3	186.4
			Tsunami	0.005	0.008	0.003	0.002	0.002	0.2	0.1
			Landslide	0.179	0.246	0.067	0.040	0.053	12.5	8.5
Osaka Prefecture	3341	15,889	Flood	0.255	0.249	−0.006	0.149	0.135	154.4	104.7
			Storm surge	0.198	0.161	−0.037	0.170	0.132	200.8	120.2
			Tsunami	0.112	0.102	−0.010	0.076	0.068	95.2	62.7
			Landslide	0.130	0.184	0.054	0.034	0.047	10.6	8.8
Shizuoka Prefecture	2713	25,140	Flood	0.386	0.310	−0.076	0.233	0.180	77.0	33.2
			Storm surge	0.087	0.052	−0.035	0.038	0.022	12.7	4.7
			Tsunami	0.136	0.112	−0.024	0.072	0.056	22.7	9.5
			Landslide	0.351	0.406	0.055	0.126	0.129	16.5	8.6
Nagano Prefecture	1396	24,994	Flood	0.144	0.135	−0.009	0.095	0.077	28.1	9.6
			Storm surge	0.000	0.000	0.000	0.000	0.000	0.0	0.0
			Tsunami	0.000	0.000	0.000	0.000	0.000	0.0	0.0
			Landslide	0.437	0.500	0.064	0.197	0.223	24.6	11.1

Note: This supplementary case-study comparison was conducted as a diagnostic analysis and was not intended as a full national reanalysis. Core-cell values were calculated using postcode-level population core-cell records, whereas all-cell values were calculated using all populated 250 m census grid cells in each selected case-study region. JPWI quartiles were not assigned to all populated cells because JPWI is defined for postcode representative points, not for all populated 250 m census grid cells. In some regions, multiple postcode-level records share the same 250 m population core cell. The difference in *HazardInclusion* was calculated as the all-cell proportion minus the core-cell proportion. The proportion of units with *HazardInclusion* = 1 indicates identified overlap in the available official hazard-zone layers and should not be interpreted as a complete estimate of hazard presence or absence. Mean *HazardExposedPopulation* per analysis unit should not be interpreted as total exposure within the selected regions.

Appendix D. Supplementary 3 × 3-Neighborhood Sensitivity Analysis

The 3 × 3-neighborhood sensitivity analysis showed JPWI-stratified patterns broadly consistent with the main core-cell analysis. The 3 × 3-neighborhood mean *HazardInclusion* proportions were similar to the main core-cell proportions. The 3 × 3-neighborhood mean *HazardCoverageRatio* values were lower than those in the main analysis because grid cells with no identified hazard-zone overlap were included in the average, but the JPWI-stratified tendencies were consistent. The average of the 3 × 3-neighborhood sums of *HazardExposedPopulation* also showed patterns consistent with the main findings, while reflecting the larger local-neighborhood spatial unit and the population-size component of

the exposure estimate. Therefore, the 3 × 3-neighborhood indicators should be interpreted as local-neighborhood hazard indicators around JPWI-classified population core cells.

Table A3. Supplementary 3 × 3-neighborhood sensitivity analysis of hazard-zone indicators by JPWI quartile.

Hazard-Zone Type	JPWI Quartile	*HazardInclusion*			Mean 3 × 3-Neighborhood *HazardCoverageRatio*	Mean 3 × 3-Neighborhood Sum of *HazardExposedPopulation*
		Core-Cell	3 × 3 Mean	Difference		
Flood inundation zones	Q1	0.190	0.190	0.001	0.076	9.7
	Q2	0.351	0.353	0.002	0.202	92.4
	Q3	0.391	0.393	0.002	0.247	432.3
	Q4	0.352	0.354	0.001	0.241	1234.8
Storm surge inundation zones	Q1	0.018	0.017	−0.001	0.008	1.3
	Q2	0.063	0.060	−0.002	0.039	21.9
	Q3	0.113	0.113	−0.001	0.081	153.1
	Q4	0.191	0.191	0.000	0.150	942.7
Tsunami inundation zones	Q1	0.087	0.085	−0.002	0.026	3.6
	Q2	0.113	0.110	−0.003	0.053	27.4
	Q3	0.133	0.133	0.000	0.075	125.9
	Q4	0.140	0.141	0.001	0.093	476.9
Landslide warning zones	Q1	0.647	0.638	−0.009	0.253	21.8
	Q2	0.357	0.353	−0.003	0.109	44.9
	Q3	0.219	0.229	0.009	0.057	87.6
	Q4	0.119	0.128	0.008	0.025	92.7

Note: The 3 × 3-neighborhood analysis was conducted as a local-neighborhood sensitivity check and was not intended to estimate total hazard-zone-based exposure within entire postcode areas. The mean 3 × 3-neighborhood *HazardInclusion* proportion represents the average proportion of grid cells with *HazardInclusion* = 1 among the population core cell itself and the surrounding grid cells with available census population data within the 3 × 3 neighborhood. The difference was calculated as the mean 3 × 3-neighborhood *HazardInclusion* proportion minus the main core-cell *HazardInclusion* proportion. The mean 3 × 3-neighborhood *HazardCoverageRatio* includes grid cells within the 3 × 3 neighborhood with no identified hazard-zone overlap. The mean 3 × 3-neighborhood sum of *HazardExposedPopulation* represents the average, across population core-cell records, of the summed estimated exposed population in the grid cells included in the 3 × 3 neighborhood. It should not be directly compared with the core-cell value as an equivalent spatial unit. JPWI quartiles refer to the JPWI value of the postcode representative point corresponding to the central population core cell. JPWI was not recalculated for the 3 × 3 neighborhood, and neighboring cells were not assigned their own JPWI values. Therefore, the 3 × 3-neighborhood indicators should be interpreted as local-neighborhood hazard indicators around JPWI-classified population core cells, not as indicators calculated over the same spatial unit as JPWI.

Appendix E. Combinations of Identified Hazard-Zone Types

As a supplementary descriptive analysis, we counted the number of identified hazard-zone types for each population core cell. This count was calculated by summing the four binary *HazardInclusion* indicators for each cell and was summarized by JPWI quartile (Table A4). This analysis was intended to describe cases in which multiple hazard-zone types were identified within the same population core cells in the available hazard-zone layers, not to assess simultaneous or compound hazard events, cumulative exposure, or compound risk.

Across all JPWI quartiles, most population core cells had either zero or one identified hazard-zone type. Cells with three or four identified hazard-zone types were relatively uncommon, although the proportion of cells with three identified hazard-zone types was higher in Q4 than in Q1. These results indicate that multiple hazard-zone types were identified within some population core cells, but the patterns should be interpreted cautiously because the four hazard-zone layers differ in scenario assumptions, designation criteria, and spatial coverage.

Table A5 reports the detailed combinations of identified hazard-zone types within population core cells. These combinations correspond to the counts of zero to four identified hazard-zone types summarized in Table A4. As with Table A4, the combinations should be interpreted as cases in which multiple hazard-zone types were identified within the same

population core cells in the available hazard-zone layers, not as evidence of simultaneous or compound hazard events, cumulative exposure, or compound risk.

Table A4. Number and percentage of identified hazard-zone types at population core cells by JPWI quartile.

JPWI Quartile	Retained Core-Cell Records, *n*	0 Types, *n* (%)		1 Type, *n* (%)		2 Types, *n* (%)		3 Types, *n* (%)		4 Types, *n* (%)	
Q1	23,226	5590	(24.1%)	13,753	(59.2%)	3560	(15.3%)	311	(1.3%)	12	(0.1%)
Q2	27,030	9024	(33.4%)	13,047	(48.3%)	4097	(15.2%)	816	(3.0%)	46	(0.2%)
Q3	27,787	10,282	(37.0%)	12,553	(45.2%)	3708	(13.3%)	1150	(4.1%)	94	(0.3%)
Q4	28,187	13,051	(46.3%)	9515	(33.8%)	3847	(13.7%)	1700	(6.0%)	74	(0.3%)

Note: The number of hazard-zone types was calculated by summing the four binary *HazardInclusion* indicators for flood inundation zones, storm surge inundation zones, tsunami inundation zones, and landslide warning zones for each population core cell. Percentages were calculated using retained cells in each JPWI quartile as the denominator. A value of 0 types indicates that no hazard-positive pixels were identified in the available hazard-zone layers and should not be interpreted as definitive absence of hazard. Because the hazard-zone layers differ in scenario assumptions, designation criteria, and spatial coverage, the counts should be interpreted as the number of hazard-zone types identified within the same population core cell, not as evidence of simultaneous or compound hazard events, cumulative exposure, or compound risk.

Table A5. Detailed combinations of identified hazard-zone types at population core cells by JPWI quartile.

Hazard-Zone Combination	No. of Types	Overall, *n* (%)		Q1, *n* (%)		Q2, *n* (%)		Q3, *n* (%)		Q4, *n* (%)	
No identified overlap	0	37,947	(35.7%)	5590	(24.1%)	9024	(33.4%)	10,282	(37.0%)	13,051	(46.3%)
Flood only	1	21,260	(20.0%)	2024	(8.7%)	6221	(23.0%)	7388	(26.6%)	5627	(20.0%)
Storm surge only	1	1633	(1.5%)	15	(0.1%)	158	(0.6%)	510	(1.8%)	950	(3.4%)
Tsunami only	1	2438	(2.3%)	374	(1.6%)	672	(2.5%)	849	(3.1%)	543	(1.9%)
Landslide only	1	23,537	(22.2%)	11,340	(48.8%)	5996	(22.2%)	3806	(13.7%)	2395	(8.5%)
Flood + storm surge	2	2908	(2.7%)	35	(0.2%)	392	(1.5%)	809	(2.9%)	1672	(5.9%)
Flood + tsunami	2	1689	(1.6%)	76	(0.3%)	353	(1.3%)	670	(2.4%)	590	(2.1%)
Flood + landslide	2	1767	(1.7%)	47	(0.2%)	258	(1.0%)	500	(1.8%)	962	(3.4%)
Storm surge + tsunami	2	5529	(5.2%)	2144	(9.2%)	2000	(7.4%)	999	(3.6%)	386	(1.4%)
Storm surge + landslide	2	475	(0.4%)	48	(0.2%)	126	(0.5%)	206	(0.7%)	95	(0.3%)
Tsunami + landslide	2	2844	(2.7%)	1210	(5.2%)	968	(3.6%)	524	(1.9%)	142	(0.5%)
Flood + storm surge + tsunami	3	2476	(2.3%)	42	(0.2%)	310	(1.1%)	688	(2.5%)	1436	(5.1%)
Flood + storm surge + landslide	3	237	(0.2%)	17	(0.1%)	60	(0.2%)	88	(0.3%)	72	(0.3%)
Flood + tsunami + landslide	3	363	(0.3%)	59	(0.3%)	106	(0.4%)	122	(0.4%)	76	(0.3%)
Storm surge + tsunami + landslide	3	901	(0.8%)	193	(0.8%)	340	(1.3%)	252	(0.9%)	116	(0.4%)
Flood + storm surge + tsunami + landslide	4	226	(0.2%)	12	(0.1%)	46	(0.2%)	94	(0.3%)	74	(0.3%)

Note: Combinations of identified hazard-zone types were defined using the four binary *HazardInclusion* indicators for flood inundation zones, storm surge inundation zones, tsunami inundation zones, and landslide warning zones. Percentages in the "Overall" column were calculated using all retained population core cells as the denominator, whereas percentages in the JPWI quartile columns were calculated using retained cells in each JPWI quartile as the denominator. "No identified overlap" indicates that none of the four *HazardInclusion* indicators equaled 1 and corresponds to 0 identified hazard-zone types in Table A4; it should not be interpreted as the definitive absence of hazard. As with Table A4, these combinations should be interpreted as cases in which hazard-zone types were identified within the same population core cells in the available hazard-zone layers, not as evidence of simultaneous or compound hazard events, cumulative exposure, or compound risk.

References

1. Tellman, B.; Sullivan, J.A.; Kuhn, C.; Kettner, A.J.; Doyle, C.S.; Brakenridge, G.R.; Erickson, T.A.; Slayback, D.A. Satellite imaging reveals increased proportion of population exposed to floods. *Nature* **2021**, *596*, 80–86. [CrossRef] [PubMed]
2. Stalhandske, Z.; de Ruiter, M.C.; Chambers, J.; Zimmermann, S.; Colón-González, F.J.; Sairam, N.; Bresch, D.N.; Kropf, C.M. Global Assessment of Population Exposure to Multiple Climate-Related Hazards from 2003 to 2021: A Retrospective Analysis. *Lancet Planet. Health* **2025**, *9*, 101295. [CrossRef] [PubMed]
3. Raduszynski, T.; Numada, M. Measure and Spatial Identification of Social Vulnerability, Exposure and Risk to Natural Hazards in Japan Using Open Data. *Sci. Rep.* **2023**, *13*, 664. [CrossRef] [PubMed]

4. Nakano, T.; Takeya, S. Demographic statistics by living situation in disaster risk areas based on population census micro data. *J. Archit. Plan.* **2024**, *89*, 854–861. (In Japanese) [CrossRef]
5. Matsuura, T.; Yanagihara, H.; Ikemoto, A.; Kazama, S.; Kawagoe, S. Assessment of Exposed Population to Fluvial Flood, Pluvial Flood, and Slope Failure Considering Climate and Population Changes across Japan. *Jpn. J. JSCE* **2025**, *81*, 24-16009. (In Japanese) [CrossRef]
6. Hada, Y.; Maeda, M. Change in Population within Estimated Flood Inundation Area in Japan and its Prefectures. *J. Disaster Inf. Stud.* **2020**, *18*, 107–114. (In Japanese) [CrossRef] [PubMed]
7. Kobayashi, T.; Katayama, A.; Hayashi, Y.; Morikawa, Y.; Hatano, Y.; Kikuchi, M. A Nationwide Quantitative Analysis of Population Changes in Flood Inundation Assumption Areas from an Urban Planning Perspective. *J. City Plan. Inst. Jpn.* **2025**, *60*, 946–952. (In Japanese) [CrossRef]
8. Honma, M.; Ushiyama, M. Estimation of the Number of People Who Need to Evacuate during Heavy Rain in Japan and Each Prefecture. *J. Disaster Inf. Stud.* **2024**, *22*, 2. (In Japanese)
9. Ochiai, T.; Enomoto, T. Multi-Hazard Evaluation Using Cluster Analysis—For Designated Evacuation Centers of Yokohama. *J. Geogr. Inf. Syst.* **2021**, *13*, 243–259. [CrossRef]
10. Venerandi, A.; Mellen, H.; Romice, O.; Porta, S. Walkability Indices—The State of the Art and Future Directions: A Systematic Review. *Sustainability* **2024**, *16*, 6730. [CrossRef]
11. De Vos, J.; Lättman, K.; van der Vlugt, A.L.; Welsch, J.; Otsuka, N. Determinants and effects of perceived walkability: A literature review, conceptual model and research agenda. *Transp. Rev.* **2022**, *43*, 303–324. [CrossRef]
12. Frank, L.D.; Sallis, J.F.; Saelens, B.E.; Leary, L.; Cain, K.; Conway, T.L.; Hess, P.M. The development of a walkability index: Application to the Neighborhood Quality of Life Study. *Br. J. Sports Med.* **2010**, *44*, 924–933. [CrossRef] [PubMed]
13. Hino, K.; Baba, H.; Kim, H.; Shimizu, C. Validation of a Japanese Walkability Index Using Large-Scale Step Count Data of Yokohama Citizens. *Cities* **2022**, *123*, 103614. [CrossRef]
14. Shimizu, C.; Baba, H.; Kawayoke, T.; Matsunawa, M. *Walkability and Real Estate Value: Development of Walkability Index*; CSIS Discussion Paper Series, No. 163; The University of Tokyo: Tokyo, Japan, 2020. Available online: https://www.csis.u-tokyo.ac.jp/wp-content/uploads/2020/06/163.pdf (accessed on 1 February 2026). (In Japanese)
15. Tanimoto, R.; Hanibuchi, T.; Nakaya, T. Development of Japan Postcode-level Walkability Index and Examination of its Usefulness. *Q. J. Geogr.* **2023**, *75*, 16–26. (In Japanese) [CrossRef] [PubMed]
16. Tanimoto, R.; Hanibuchi, T.; Nakaya, T. *Japan Postcode-Level Walkability Index (JPWI)*; The Tohoku Geographical Association: Sendai, Japan, 2023. [CrossRef]
17. Oya, S.; Nakamura, K. The Relationship of QOL and Walkability Considering Urban Disaster Resilience. *J. Jpn. Soc. Civ. Eng. Ser. D3 (Infrastruct. Plan. Manag.)* **2022**, *77*, I_765–I_776. (In Japanese) [CrossRef] [PubMed]
18. Gorzka, J.; Burda, I.; Nyka, L. Walkability and Flood Resilience: Public Space Design in Climate-Sensitive Urban Environments. *Urban Plan.* **2025**, *10*, 9561. [CrossRef]
19. Porębska, A.; Rizzi, P.; Otsuki, S.; Shirotsuki, M. Walkability and Resilience: A Qualitative Approach to Design for Risk Reduction. *Sustainability* **2019**, *11*, 2878. [CrossRef]
20. Kim, H.; Baba, H.; Shimizu, C.; Hino, K. The relationship of single-family detached house prices with neighborhood walkability and disaster risk. *PLoS ONE* **2023**, *18*, e0292657. [CrossRef] [PubMed]
21. Kanamori, T.; Yan, W. Walkability Assessment of Elderly People in Collective Relocation after the Great East Japan Earthquake—A Case Study in Kesennuma City, Japan. In Proceedings of the REAL CORP 2022: Mobility, Knowledge and Innovation Hubs in Urban and Regional Development, Vienna, Austria, 14–16 November 2022; pp. 893–902.
22. United Nations. *Transforming Our World: The 2030 Agenda for Sustainable Development*; United Nations: New York, NY, USA, 2015. Available online: https://sdgs.un.org/2030agenda (accessed on 22 March 2026).
23. United Nations Office for Disaster Risk Reduction (UNISDR). *Sendai Framework for Disaster Risk Reduction 2015–2030*; UNISDR: Geneva, Switzerland, 2015. Available online: https://www.undrr.org/publication/sendai-framework-disaster-risk-reduction-2015-2030 (accessed on 22 March 2026).
24. Hazard Map Portal Site (Open Data). Geospatial Information Authority of Japan. Available online: https://disaportal.gsi.go.jp/hazardmapportal/hazardmap/copyright/opendata.html (accessed on 31 January 2026).
25. The 250 Meter Population Grid Data from the 2020 Population Census, the Portal Site of Official Statistics of Japan (e-Stat). Available online: https://www.e-stat.go.jp/gis/statmap-search?page=1&type=1&toukeiCode=00200521&toukeiYear=2020&aggregateUnit=H&serveyId=H002005112020&statsId=T001141&datum=2011 (accessed on 31 January 2026).
26. Utsu, K. *Japan 250-Meter Grid Hazard-Zone and Population Exposure Dataset: Hazard Areal Coverage and Estimated Exposed Population (Version 2.0) [Data Set]*; Zenodo: Geneva, Switzerland, 2026. [CrossRef]
27. Utsu, K. *Japan 250-Meter Grid Hazard-Zone and Estimated Population Exposure Dataset: Postcode-Level Population Core Cell Subset [Data Set]*; Zenodo: Geneva, Switzerland, 2026. [CrossRef]

28. Cabinet Office (Disaster Management). Guidelines on Evacuation Information. 2022. Available online: https://www.bousai.go.jp/oukyu/hinanjouhou/r3_hinanjouhou_guideline/pdf/hinan_guideline.pdf (accessed on 21 February 2026). (In Japanese)
29. Japan Meteorological Agency (JMA). Earthquake! Tsunami! Evacuate Immediately! Leaflet (EN). Available online: https://www.jma.go.jp/jma/kishou/know/jishin/tsunami_bosai/img/leaflet_tsunami_bosai_en.pdf (accessed on 21 February 2026).
30. Fire and Disaster Management Agency (FDMA). Important Information on Countermeasures Against Earthquake Disasters—"Evacuate on Foot, If Possible". Available online: https://www.fdma.go.jp/relocation/bousai_manual/e/lat/later33.html (accessed on 21 February 2026).
31. Ministry of Land, Infrastructure, Transport and Tourism (MLIT). *[Landslide Disaster Evacuation Guideline]*; MLIT: Tokyo, Japan, 2015. Available online: https://www.mlit.go.jp/report/press/sabo01_hh_000016.html (accessed on 21 February 2026).

Disclaimer/Publisher's Note: The statements, opinions and data contained in all publications are solely those of the individual author(s) and contributor(s) and not of MDPI and/or the editor(s). MDPI and/or the editor(s) disclaim responsibility for any injury to people or property resulting from any ideas, methods, instructions or products referred to in the content.